Vol. 68 • No. 10

October 2025

Microwave Journal®

horizon house®

Founded in 1958

mwjournal.com

MILLER MMIC

Advancing RFIC Design Through Human-AI collaboration and competition

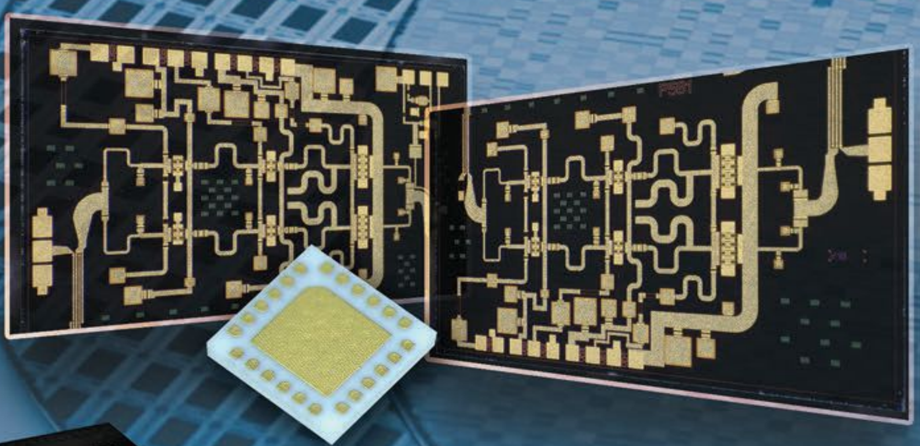

Miller MMIC is a global provider of RF semiconductor solutions with expertise in GaAs and GaN processes. We offer a diverse range of products tailored to various wireless applications. Our product lineup encompasses a wide array of offerings, including Low Noise Amplifiers, Distributed Amplifiers, Power Amplifiers, Driver Amplifiers, RF Switches, RF PIN Diode Switches, and numerous other voltage- and digitally-controllable RF components.

QFN and SiP (System-In-Package) available

RF Distributed Low Noise Amplifiers

PN	Freq Low (GHz)	Freq High (GHz)	Gain (dB)	NF(dB)	P1dB (dBm)	Voltage (VDC)	Current (mA)	Package
MMW001T	DC	20.0	17~19	1~3.5	23 @ 10GHz	8.0	145	die
MMW4FP	DC	50.00	16.00	4.00	24.00	10	200	die
MMW507	0.20	22.0	14.0	4 - 6	28.0	10.0	350	die
MMW508	DC	30.0	14.0	2.5dB @ 15GHz	24.5	10.0	200	die
MMW509	30KHz	45.0	15.0		20.0	6.0	190	die
MMW510	DC	45.0	11.0	4.5	15.5	6.0	100	die
MMW510F	DC	30.00	20.00	2.50	22.00			die
MMW511	0.04	65.0	10.0	9.0	18.0	8.0	250	die
MMW512	DC	65.0	10.0	5.0	14.5	4.5	85	die
MMW5FN	DC	67.00	14.00	2.00	19.00	4.5	81	die
MMW5FP	DC	67.00	14.00	4.00	21.00	8	140	die
MMW011	DC	12.0	14.0		30.5	12.0	350	die

Low Noise Amplifiers

PN	Freq Low (GHz)	Freq High (GHz)	Gain (dB)	NF(dB)	P1dB (dBm)	Voltage (VDC)	Current (mA)	Package
MML040	6.0	18.0	24.0	1.5	14.0	5.0	35	die
MML058	1.0	18.0	15.0	1.7	17.0	5.0	35	die
MML063	18.0	40.0	11.0	2.9	15.0	5.0	52	die
MML080	0.8	18.0	16.5/15.5	1.9/1.7	18/17.5	5.0	65/40	die
MML081	2.0	18.0	25/23	1.0/1.0	16/9.5	5.0	37/24	die
MML083	0.1	20.0	23.0	1.6	11.0	5.0	58	die

RF Driver Amplifier

PN	Freq Low (GHz)	Freq High (GHz)	Gain (dB)	NF(dB)	P1dB (dBm)	Voltage (VDC)	Current (mA)	Package
MM3006	2.0	20.0	19.5	2.5	22.0	7.0	130	die
MM3014	6.0	20.0	15.0	-	19.5	5.0	107	die
MM3017T	17.0	43.0	25.0		22.0	5.0	140	die
MM3031T	20.0	43.0	20.0		24.0	5.0	480	die
MM3051	17.0	24.0	25.0	-	25.0	5.0	220	die
MM3058	18.0	40.0	20/19.5	2.5/2.3	16/14	5/4	69/52	die
MM3059	18.0	40.0	16/16	2.5/2.3	16/15	5/4	67/50	die

GaAs Medium Power Amplifier

PN	Freq Low (GHz)	Freq High (GHz)	Gain (dB)	P1dB (dBm)	Psat (dBm)	Voltage (VDC)	Current (mA)	Package
MMP107	17.0	21.0	19.0	30.0	30.0	6.0	400	die
MMP108	18.0	28.0	14.0	31.5	31.0	6.0	650	die
MMP111	26.0	34.0	25.5	33.5	33.5	6.0	1300	die
MMP112	2.0	6.0	20.0	31.5	32.0	8.0	365	die
MMP501	20.0	44.0	15.0	27 -- 32	29 - 34	5.0	1200	die
MMP502	18.0	47.0	14.0	28.0	30.0	5.0	1500	die

PN: MMW5FP

RF GaAs MMIC DC-67GHz

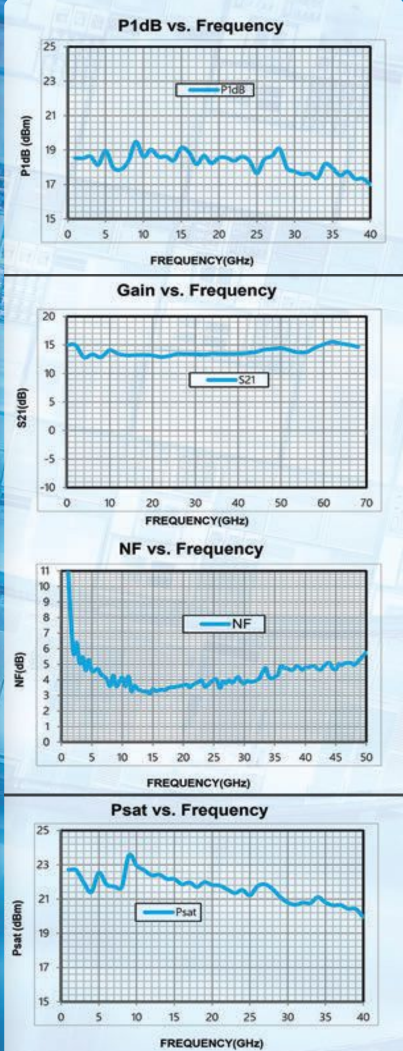

CALL US 1-833-2MILLER(264-5537)
WWW.MILLERMMIC.COM

MILLER MMIC

sales@millermmic.com
support@millermmic.com

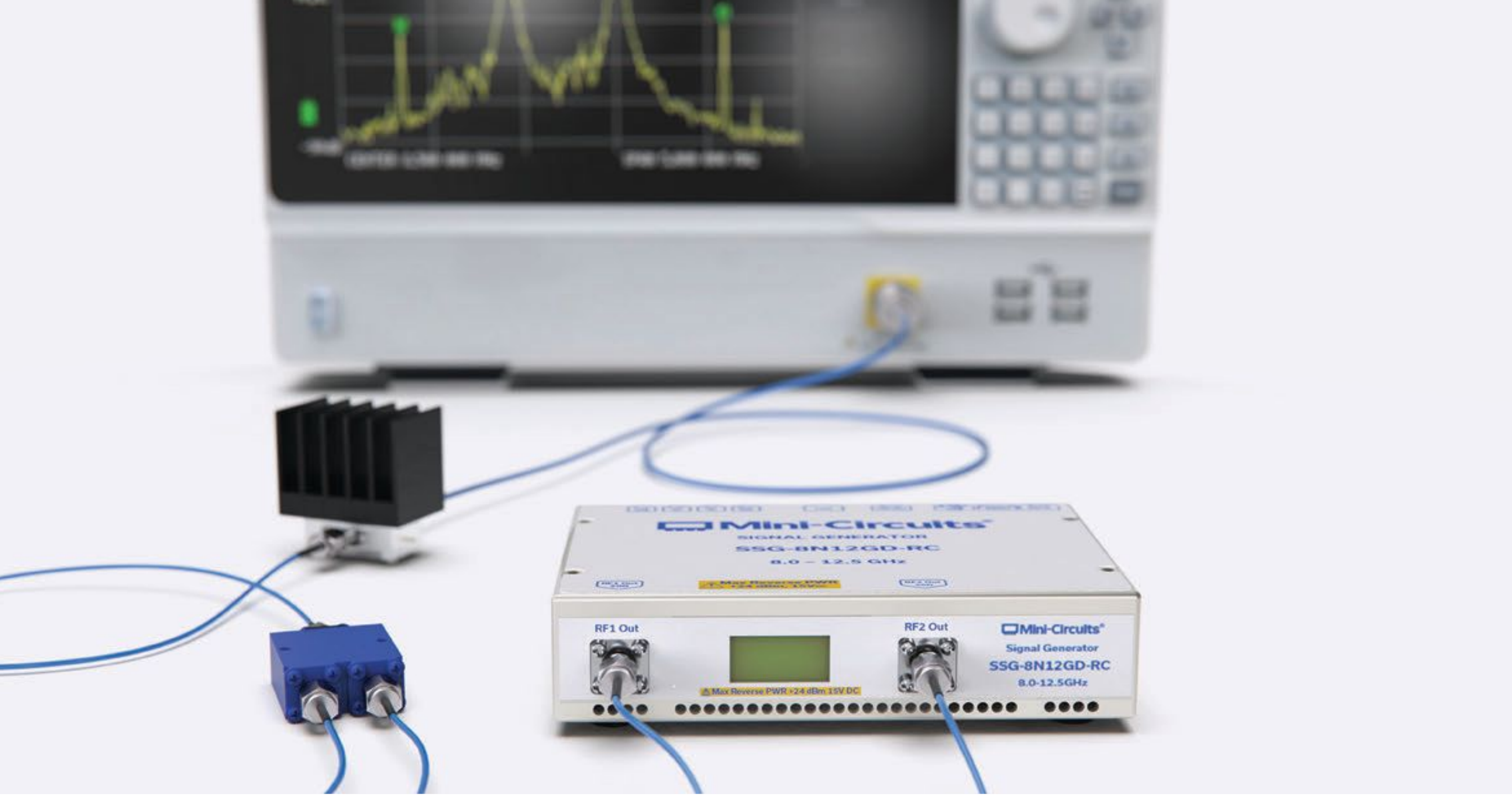

SSG SERIES

Signal Generators

Single-Channel & Dual Channel

LEARN MORE

Highlights

- Wide output power range
- Dual outputs with 360° independent phase control
- Pulsed, CW, AM, FM, and chirp modulations
- USB, Ethernet & PoE control interfaces
- Daisy chain port for multi-module control
- Compact housing, 3.6 x 5.1 x 1.2″

Model Number	Frequency	Output Power	# Channels	Release Status
SSG-8N12G-RC	8 to 12.5 GHz	-55 to 23 dBm	1	Production
SSG-8N12GD-RC	8 to 12.5 GHz	-55 to 23 dBm	2	Production
SSG-5N9G-RC	5 to 9 GHz	-55 to 23 dBm	1	Production
SSG-5N9GD-RC	5 to 9 GHz	-55 to 23 dBm	2	Production
SSG-9G-RC	0.01 to 9 GHz	-50 to 15 dBm	1	Q2, 2025
SSG-9GD-RC	0.01 to 9 GHz	-50 to 15 dBm	2	Q2, 2025
SSG-R7N6G-RC	0.7 to 6 GHz	-55 to 23 dBm	1	Q2, 2025
SSG-R7N6GD-RC	0.7 to 6 GHz	-55 to 23 dBm	2	Q3, 2025
SSG-1R5G-RC	0.02 to 1.5 GHz	-55 to 23 dBm	1	Q3, 2025
SSG-1R5GD-RC	0.02 to 1.5 GHz	-55 to 23 dBm	2	Q3, 2025

PWR SERIES

Power Sensors

Turn Your PC into a High-Performance Power Meter

LEARN MORE

- Dynamic range options spanning -60 to +20 dBm
- CW, true RMS, peak and average measurement capability
- Sample rates up to 80 million samples per second
- 50 and 75Ω models
- Software package supports automated measurement with statistical analysis and time domain plots
- No external calibration required

Model #	Control Interface	Measurement Type	Freq. Range (MHz)	Input Power Range (dBm)	Measurement Speed (ms)
PWR-40PW-RC	USB & Ethernet	Peak & Avg.	500-40000	-20 to 20	5.00E-05
PWR-18PWHS-RC	USB & Ethernet	Peak & Avg.	50-18000	-60 to 20	1.30E-05
PWR-18RMS-RC	USB & Ethernet	RMS	50-18000	-60 to 20	0.5
PWR-9PWHS-RC	USB & Ethernet	Peak & Avg.	50-9000	-60 to 20	0.000013
PWR-9RMS-RC	USB & Ethernet	RMS	50-9000	-60 to 20	0.5
PWR-8P-RC	USB & Ethernet	Peak & Avg.	10-8000	-60 to 20	0.002
PWR-8FS	USB	CW	1-8000	-30 to 20	10
PWR-8GHS	USB	CW	1-8000	-30 to 20	30
PWR-8GHS-RC	USB & Ethernet	CW	1-8000	-30 to 20	30
PWR-8PW-RC	USB & Ethernet	Peak & Avg.	10-8000	-60 to 20	0.00005


Innovate.
Advance.
Repeat.
Breakthrough products featuring smaller footprints,
higher frequencies, greater thermal stability, and rapid delivery
Ultraminiature High Q Filters
to 10 GHz, custom diplexers
and multiplexers available
Tunable Gain Equalizer
to 50 GHz. Linear, parabolic
and ripple removal
Cryogenic Attenuators
SMT and coax models,
operate reliably at 4 mK
Filtered 38999 Connectors
3 pin configurations
12-week delivery
Get more details and see the full line-up of innovative new products at
spectrumcontrol.com/new25Q3
SPECTRUM
CONTROL
spectrumcontrol.com © 2025 Spectrum Control, Inc. All rights reserved


RF-LAMBDA
THE LEADER OF RF BROADBAND SOLUTIONS
BROADBAND SSPA / EMC BENCHTOP
SOLID STATE POWER AMPLIFIER
0.1-22GHZ
ULTRA BROADBAND SSPA
RFLUPA01M22GA
4W 0.1-22GHZ
RFLUPA0218GB
20W 1-19GHZ
6-18GHZ 800W
CW REMC06G18GG
18-40GHZ 200W
CW REMC18G40GQ
0. 1-6GHZ VHZ,
UHF, L, S, C BAND
RFLUPA02G06GC
100W 2-6GHZ
RFLUPA0706GD
30W 0.7-6GHZ
MADE IN
USA
6-18GHZ C, X, KU BAND
RFLUPA08G11GA
50W 8-11GHZ
RFLUPA0618GD
60W 6-18GHZ
RFLUPA06G12GB
25W 6-12GHZ
18-50GHZ K, KA, V BAND
RFLUPA18G47GC
2W 18-47GHZ
RFLUPA27G34GB
15W 27-34GHZ
RFLUPA47G53GA2
10W 47-53GHZ
RFLUPA27G34GB
30W 18-40GHZ
BENCHTOP RF MICROWAVE SYSTEM POWER AMPLIFIER
REMC02G06GE
600W 2-6GHZ
REMC18G40GC2
40W 18-40GHZ
RAMP30G65GG
8W 30-65GHZ
RAMP06G18GA
10W 6-18GHZ
RAMP00M65GA
DC-65GHZ
www.rflambda.com
sales@rflambda.com
1-888-976-8880
1-972-767-5998
San Diego, CA, US
Carrollton, TX, US
Ottawa, ONT, Canada
Frankfurt, Germany

Microwave Journal

CONTENTS

October 2025
Vol. 68 • No. 10
Passive Components &
Integrated Assemblies
mwjournal.com

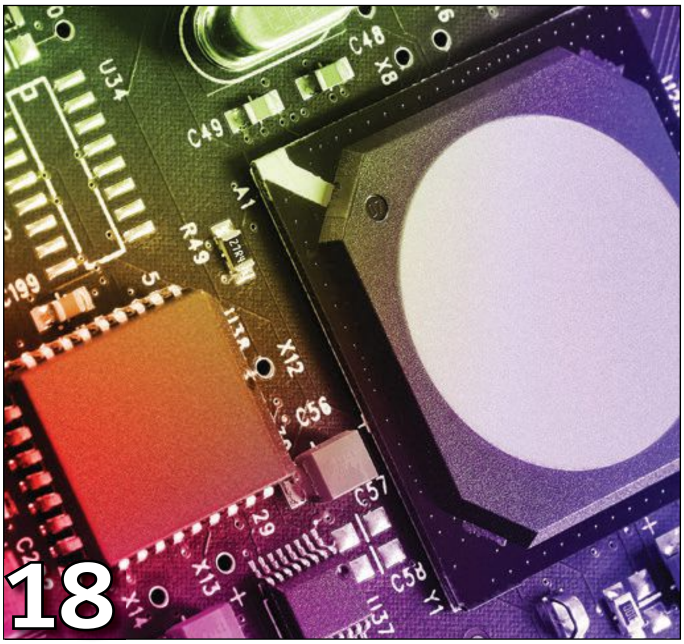

online spotlight

Look for this month's exclusive article online at mwjournal.com

LCP-Based 24 GHz Bandpass Filter with Wide Rejection Band up to 110 GHz

Chu-Yu Chen, Department of Electrical Engineering, National University of Tainan, Taiwan and Wei-Ting Lee, Kun-Yen Tu and Sin-Siang Wang, QuantumZ Inc., Taiwan

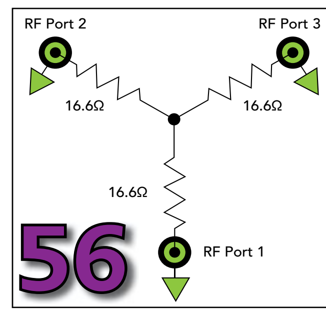

Cover Feature

MWJ Perspective

Technical Features

68 YEARS OF PUBLISHING EXCELLENCE

CONTENTS

mwjournal.com

Product Features

Tech Brief

Departments

Microwave Journal (USPS 396-250) (ISSN 0192-6225) is published monthly by Horizon House Publications Inc., 685 Canton St., Norwood, MA 02062. Periodicals postage paid at Norwood, MA 02062 and additional mailing offices.

POSTMASTER: Email address corrections to mwj@e-circ.net.com. Subscription information: (978) 671-0446. This journal is issued without charge upon written request to qualified persons working in the RF & microwave industry. Other subscriptions are: domestic, $130.00 per year, two-year subscriptions, $200.00; foreign, $225.00 per year, two-year subscriptions, $400.00; back issues (if available) and single copies, $20.00 domestic and $30.00 foreign. Claims for missing issues must be filed within 90 days of date of issue for complimentary replacement.

STAFF

Group Director: Carl Sheffres
Associate Publisher: Michael Hallman
Media Director: Patrick Hindle
Brand & Content Director: Jennifer DiMarco
Technical Editor: Del Pierson
Associate Technical Editor: Cliff Drubin
Editorial & Media Specialist: Kelley Roche
Associate Editor: Kaitlyn Joyner
Multimedia Staff Editor: Barbara Walsh
Electronic Marketing Manager: Chris Stanfa
Senior Digital Content Specialist: Lauren Tully
Digital Content Specialist: Vincent Carrabino
Director of Production & Distribution: Edward Kiessling
Art Director: Janice Levenson
Graphic Designer: Ann Pierce

EUROPE

Office Manager: Nina Plesu

CORPORATE STAFF

CEO: William M. Bazzy
President: Ivar Bazzy
Vice President: Jared Bazzy

EXECUTIVE EDITORIAL OFFICE

685 Canton Street, Norwood, MA 02062
Tel: (781) 769-9750
FAX: (781) 769-5037
e-mail: mwj@mwjournal.com

EUROPEAN EDITORIAL OFFICE

16 Sussex Street, London SW1V 4RW, England
Tel: Editorial: +44 207 596 8730 Sales: +44 207 596 8740
FAX: +44 207 596 8749

SUBSCRIPTION SERVICES

Send subscription inquiries and address changes to:
Tel: (978) 671-0446
e-mail: mwj@e-circ.net

www.mwjournal.com

Printed in the USA

Microwave Journal ONLINE .COM

LEARNING CENTER

Access webinars on-demand from the archived webinars and events page at www.mwjournal.com/events

WHITE PAPERS

NSI MI

Near-Field Antenna Pattern Measurements with a Streaming Digital Receiver

SIGLENT

Signal Generator Guide

Look for additional content from:

Mini-Circuits

WÜRTH ELEKTRONIK MORE THAN YOU EXPECT

eBooks

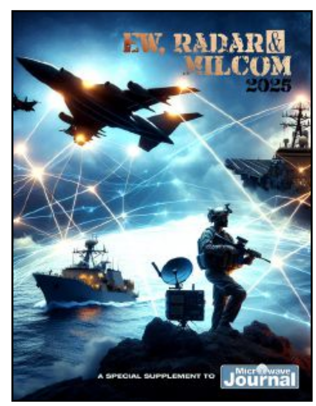

Join Us Online

Follow us @Pathindle @MWJEditor

Join us at the RF and Microwave Community

Become a fan at facebook.com/microwavejournal

Catch *Frequency Matters*, the industry update from *Microwave Journal*, microwavejournal.com/FrequencyMatters

Visit us @ mwjournal.com

MARK YOUR CALENDAR

STAY CONNECTED TO COMING EVENTS

OCTOBER

12-15
BCICTS
Scottsdale, Ariz.
https://bcicts.org/

27-30
IEEE RFID-TA
Valence, France
https://2025.ieee-rfid-ta.org/

NOVEMBER

2-7
AMTA
Tucson, Ariz.
https://2025.amta.org

3-6
Global MilSatCom
London, U.K.
www.smgconferences.com/defence/uk/conference/global-milsatcom

18-20
Space Tech Expo EU
Bremen, Germany
www.spacetechexpo-europe.com

Register online at mwjournal.com

ONLINE PANEL SERIES

11/12
5G/6G Advances

DECEMBER

2-5
APMC 2025
Jeju, South Korea
www.apmc2025.org

6-10
IEDM 2025
San Francisco, Calif.
www.ieee-iedm.org/

9-11
AOC 2025
National Harbor, Md.
https://aoc2025.org/

14-18
MAPCON 2025
Kochi, Kerala, India
https://ieeemapcon.org/

JANUARY

6-9
CES 2026
Las Vegas, Nev.
www.ces.tech

18-21
IEEE Radio & Wireless Week
Los Angeles, Calif.
https://www.radiowirelessweek.org/

Call for Papers Deadlines

10/31 CS Mantech

11/14 German Microwave Conference

FOR DETAILS VISIT MWJOURNAL.COM/EVENTS

Filtering the Future: Passive Components for 5G and 6G

Sam Suresh.J, A.Senthilkumar and G.Soundarya
Dr. Mahalingam College of Engineering and Technology, Pollachi, India

As higher data rate communication emerges, there will be extraordinary growth of 5G mmWave filters from $0.1 billion in 2024 to an expected $1.39 billion by 2033 with a CAGR of 35.8 percent.[1] This growth indicates the critical importance of these components in next-generation wireless infrastructure. With the progression toward 6G systems operating at frequencies above 100 GHz, the design and development of microwave filters encounter increasingly challenging requirements, necessitating the adoption of advanced and innovative engineering solutions.

The mmWave spectrum, particularly the 5G new radio (NR) frequency bands including n257 (28 GHz), n258 (26 GHz), n260 (39 GHz) and n261 (27 GHz), presents unique propagation characteristics and technical requirements. 6G technology focuses on faster and smarter communication. One of the frequency ranges is the D-Band (110 to 170 GHz), which supports the transfer of massive data quickly. Another range is the sub-terahertz range (100 to 300 GHz), which is useful for both high speed, short-distance communication and advanced sensing, such as gesture recognition or 3D imaging. It also faces signal loss, which has prompted researchers to work vigorously on integrated optical-wireless systems that combine the speed of optical fiber with the flexibility of wireless signals.

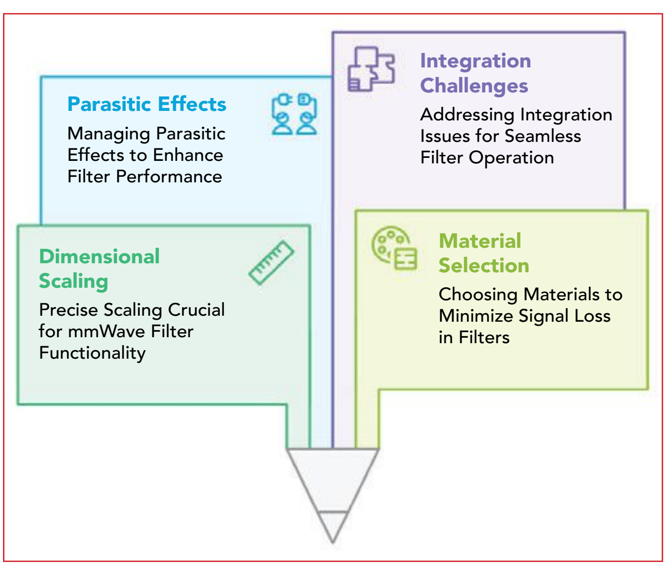

Fig. 1 **Design challenges of mmWave filters.**

mmWave filters are important passive components in both 5G and 6G communication systems due to their precise signal selection and interference suppression at high frequencies. As communication progresses into the mmWave bands (above 24 GHz for 5G and beyond 100 GHz for 6G), filters are essential to isolate the frequency channels. This is important due to higher signal attenuation, dense spectrum usage and increased sensitivity to noise and interference. They also support multiband and wideband operation, which helps achieve high data rates and low latency assured by 5G and 6G systems. Without effective filtering, hardware constraints, out-of-band noise and signal overlap would cause the performance to deteriorate. As a result, filters are crucial to maintain the selectivity, speed and dependability of sophisticated wireless communication systems.

A comprehensive analysis of current mmWave filter technologies is provided in this article, with a focus on design strategies, performance tradeoffs and emerging trends that will impact the advancement of 5G and 6G communications.

DESIGN CHALLENGES

Developing filters at mmWave frequencies presents several challenges due to the exclusive behaviour of electromagnetic waves at high frequencies. ***Figure 1*** depicts the critical design challenges of mmWave filters.

Scaling and Manufacturing Tolerances

At lower frequencies, manufacturing tolerances are generally negligible, whereas at mmWave


The only
QPL Certified
MECHANICAL
SWITCH
House!
Quick Turn
RF FILTER
Prototypes
are in our DNA!
Huge Library
of PASSIVES
with Best in Show
HIGH POWER
COUPLER
offering!
L-4241A
S/N 2206001
RUGGED & RELIABLE
AGILE & ADAPTIVE
HIGH POWER & VARIETY
RLC
RF MECHANICAL SWITCHES,
RF FILTERS & RF PASSIVES
AS9100 CERTIFIED, MADE IN USA
High Performance Precision Microwave Components
Serving the world-wide aerospace & defense community since 1959
Robust Catalog Portfolio - no hassle, quick turn, custom solutions our specialty
RLC Electronics | 83 Radio Circle, Mt. Kisco, NY 10549 | 914-241-1334 | sales@rlcelectronics.com | www.rlcelectronics.com

frequencies, they become critical design parameters. For a 28 GHz filter, variations of ±10 μm in critical dimensions can shift the center frequency by several hundred MHz. This necessitates the utilization of advanced lithographic processes with sub-micron resolution, tight control of substrate thickness variations (±5 μm), precise via diameters and pitch control in multilayer structures.

Material Selection and Loss Mechanisms

Due to the greater influence of conductor and dielectric losses, identifying suitable substrate materials becomes crucial at mmWave frequencies.

To guarantee low signal attenuation and excellent filter performance, low loss substrates are essential. Commonly used materials include Rogers RT/Duroid 5880 with a dielectric constant (ε_r) of 2.2 and a loss tangent (tan δ) of 0.0009,[2] liquid crystal polymer (LCP) with ε_r = 3.0 and tan δ = 0.002,[3] fused silica glass (ε_r = 3.8, tan δ = 0.0001) and AlN ceramics (ε_r = 8.8, tan δ = 0.0001).

Due to the skin effect, the conductor loss plays a vital role in mmWave filters. At 28 GHz, the skin depth in copper reduces to approximately 0.35 μm, making the surface roughness of conductors a significant contributor to the overall loss. To mitigate this, advanced metallization techniques are employed, such as electroplated gold surfaces for ultra-low loss, chemical-mechanical polishing for surface planarization and the use of silver-based conductors to enhance conductivity.[4,5] These measures collectively help in maintaining filter efficiency and performance at mmWave frequencies.

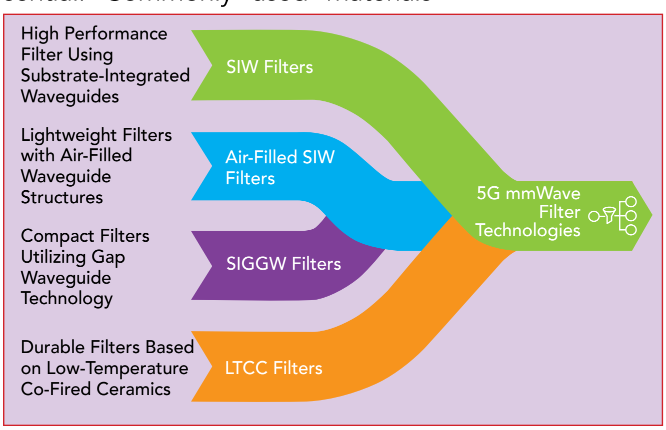

Fig. 2 Various 5G mmWave filter technologies.

Parasitic Effects and Coupling

At mmWave frequencies, parasitic effects and undesirable coupling will reduce the filter's performance. Package parasitic effects like bond wire inductance are non-negligible and should be carefully modelled, as they will provide undesirable reactance in the component. Another consideration is the via discontinuities in multilayer structures, as they introduce spurious resonances and unwanted coupling paths.[4] This degrades the filter response. Radiation loss and insufficient shielding require robust electromagnetic isolation.

Integration Challenges

The progression towards high performance 5G/6G systems leads to new issues in integration. When filters and amplifiers are designed together, impedance matching and overall system stability must be considered.[6] Integration of antennas and filters reduces the size and insertion loss but enhances the complexity.[7] System-on-package (SoP) is a technique widely used to integrate numerous RF components, such as filters, mixers and amplifiers in a single module.[8] However, this density requires well-organized thermal management methodologies to dissipate heat and to avoid a decline in functionality due to the temperature rise.[9] To ensure the dependability and effectiveness of mmWave front-end modules, these issues must be addressed.

FILTER TECHNOLOGIES FOR 5G

There are various technologies used to develop 5G mmWave filters. The prominent technologies are depicted in ***Figure 2***.

SIW Filters

The substrate-integrated waveguide (SIW) is a technology that offers excellent performance at mmWave frequencies. It integrates the low loss characteristics of conventional waveguides with the compactness of a planar circuit. A cross-coupled SIW filter at 28 GHz with 600 MHz bandwidth and three transmission zeros was developed.[10] The filter consists of an oversized cavity and a cascaded triplet. The oversized cavity provides a transmission zero (TZ) in the lower band due to the interaction of higher/lower order modes. In contrast, the cascaded triplet provides two TZs in the upper stopband. The in-band return loss is more than 15 dB, and the insertion loss is 2.7 dB. A SIW bandpass filter centered at 25.25 GHz was designed by J.-M. Huang et al., using six resonant cavities.[11] Magnetic coupling was accomplished between the cavities by adjusting the opening between them. The filter exhibited a passband from 24.8 to 25.7 GHz with an insertion loss of 0.88 dB and return loss better than 12 dB. The fabricated prototypes of both filters are shown in ***Figure 3***.

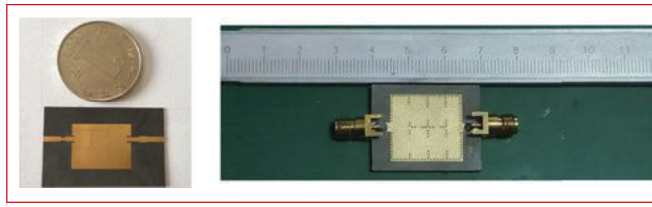

▲ Fig. 3 **Cross-coupled SIW BPF[10] and six-cavity SIW BPF.[11]**

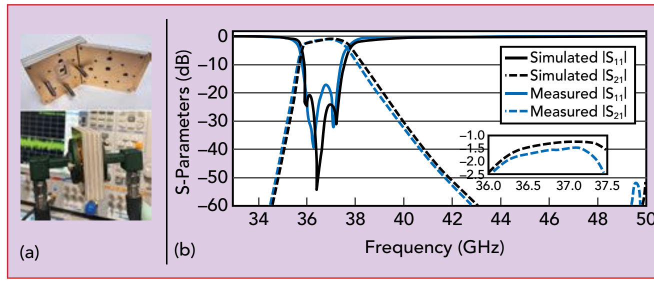

▲ Fig. 4 **(a) Assembly and measurement setup (b) Filter response.**

Air-Filled SIW Filters

This technology reduces the dielectric loss by utilizing an air-filled SIW (AFSIW) structure. This helps reduce the weight of the component while maintaining the performance, making it more suitable for aerospace and mobile applications. This variant reduces the insertion loss compared to the conventional dielectric-filled SIW techniques.

A fifth-order Chebyshev bandpass filter developed using AFSIW technology was developed by researchers.[12] Iris inductive coupling topology was used to develop the filter based on the K-inverted model and Marcuvitz design flow. It has a fractional bandwidth (FBW) of 2.98 percent centered at 27.92 GHz and an insertion loss of 1.15 dB. For comparison, the researchers also evaluated a dielectric-filled SIW filter, which exhibited a higher insertion loss of 2.13 dB. An AFSIW filter was developed using non-resonant structures between the resonators. Although AFSIW technology is technically greater in terms of loss and bandwidth, researchers face challenges such as complex manufacturability and packaging difficulties.[13]

A cavity stacked contactless air-filled (CLAF) SIW BPF was developed.[14] It supports multiple layers and has a robust assembly. It was a fourth-order filter with four stacked cavities utilizing irises for coupling. The iris layers were manufactured by metallizing the slot edges of a PCB, whereas the cavity layers were implemented using CLAF-SIW. The filter has a passband from 36 to 37.5 GHz. ***Figure 4a*** shows the filter assembly and the measurement setup and ***Figure 4b*** shows the response of the filter under test.

SIGGW Filters

A substrate-integrated gap groove waveguide (SIGGW) is an advanced planar waveguide technology. It features a perfect magnetic conductor formed by periodic vias and metallic patches on the top layer, a gap layer apidRF

World's 1st AI Driven RFIC

DESIGN PLATFORM

A PUSH-BUTTON GDS TAPE-OUT READY SOLUTION

END APPLICATIONS CUSTOMERS

PERFORMANCE-DRIVEN FOCUS
EXPANDED DESIGN CHOICES
ENHANCED SECURITY AND CONFIDENTIALITY
REDUCED DEPENDENCE ON IC VENDORS
SIGNIFICANT COST SAVINGS

SEMICONDUCTOR COMPANIES

HUGE DESIGN COST REDUCTION
TAILORED TO CUSTOMER NEEDS
100X, 1000X FASTER
SUCCESSFUL RATE INCREASE

apidRF

TRULY ENABLES A "**DIRECT INTERACTION**" MODEL FOR THE RFIC INDUSTRY ACROSS EVERY SECTOR.

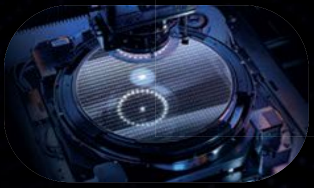

FOUNDRIES

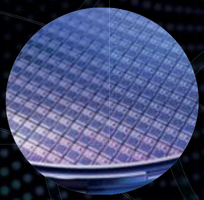

HIGHER REVENUE GREATER DESIGN VOLUME
EXPANDED CUSTOMER BASE LOWERING DESIGN ENTRY BARRIERS
ACCELERATED PRODUCT ITERATION

SIMPLE 3 STEPS

- LOGIN WWW.RAPIDRF.AI
- ENTER DESIGN TARGET
- PRESS "GENERATE"

A TAPE-OUT-READY GDS FILE WILL BE GENERATED AND **AVAILABLE FOR DOWNLOAD.**

in the middle for wave propagation and a metallic bottom layer. It utilizes grooves and conductive posts to transmit EM waves through the air-filled gap, which rejects the need for solid dielectric material. As a result, it offers lower loss and a high Q factor.

A dual-post SIW filter was designed using SIGGW technology, with overall dimensions of 2.16 λ_0 × 0.74 λ_0 × 0.16 λ_0.[15] It consisted of 12 posts (arranged in a 6 x 2 configuration) spaced at half-wavelength distance. The taller posts acted as inductive reactance, whereas the shorter posts acted as capacitive reactance, altogether forming an effective LC resonant structure. It enabled control over the TZs. The filter has a center frequency of 28 GHz with an FBW of 5 percent and an insertion loss of 1.8 dB.

LTCC-Based SIW Filters

A low-temperature co-fired ceramic (LTCC) is a multilayer ceramic fabrication technology. LTCC-based SIW filters blend the advantages of substrate-integrated waveguide with the LTCC's outstanding high frequency properties. The key advantages include low dielectric loss, multilayer integration capability, hermetic packaging for rough environments and more. An mmWave SIW filter based on LTCC was developed.[16] The structure consisted of via arrays mounted in SIW to replace the E-plane iris in the rectangular waveguide. The filter has a passband from 34.1 to 35.9 GHz, with an insertion loss of 1.8 dB and return loss of more than 21 dB. A compact SIW LTCC BPF based on capacitively loaded cavities measuring an overall dimension of 3.35 mm × 2.10 mm × 0.66 mm.[17] The CPW fed filter has a center frequency at 28 GHz with 8 percent FBW. The filter has CPW fed structures and four SIW cavity resonators. An inductive window enabled coupling between R1 and R4, as well as between R2 and R3. The circular slot provided electrical coupling between R4 and R3, whereas the pair of fan-shaped slots provided magnetic coupling between R1 and R2. Based on the coupling, the filter generated two TZs at the stopband. ***Figure 5*** depicts the filter geometry and its frequency response.

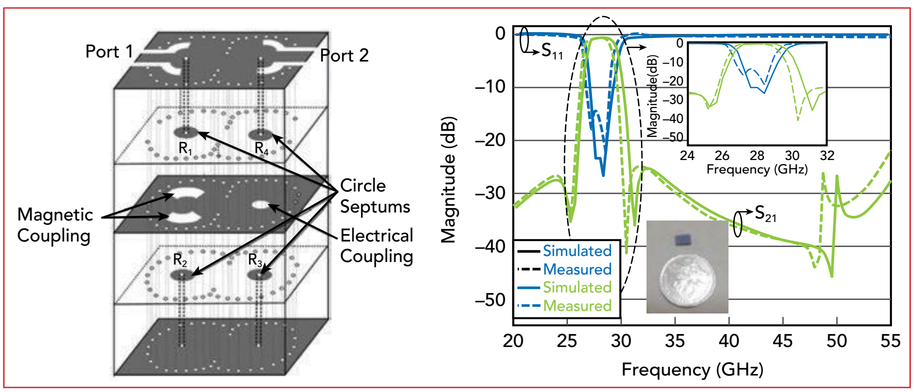

Fig. 5 Visual decomposition of the filter and its response.[17]

FILTER TECHNOLOGIES FOR 6G

Innovative filters will be developed for use in the terahertz field as part of the 6G wireless communication system. They are significant components in the RF front end. There are various techniques applied to the design and development of 6G filters, as shown in ***Figure 6***.

SIW Filters

Rogers materials, like RO4003C, have a loss tangent value of 0.0027 at 10 GHz. For higher frequencies, losses become substantial, which degrades the filter's performance. Additionally, at THz, the ohmic loss also increases due to the lower value of skin depth. Another challenge is the via spacing, which should be very small, making it difficult to achieve in the PCB process. Hence, for higher frequencies, it is advisable to use high-performance substrates such as Si, SiC or ceramics. A third-order SIW BPF on a 100 µm thick SiC substrate was demonstrated.[18] The filter has three cavities, in which cavities 1 and

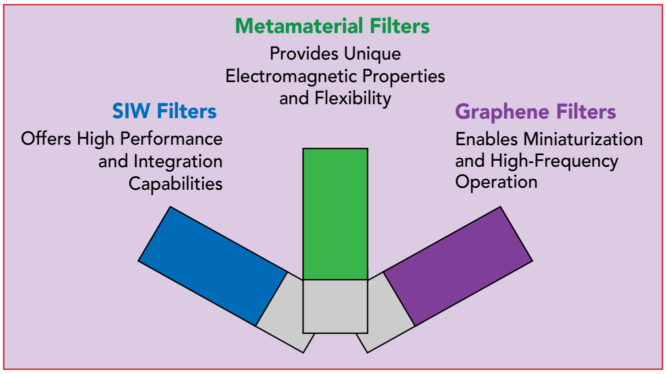

Fig. 6 Technologies for 6G filter development.

3 operate at the TE_{101} mode and cavity 2 functions at the TE_{103} mode. Cavity 2 was larger, which provided a wider coupling window between the other cavities and hence resulted in a wider bandwidth and higher Q factor. The filter has a passband centered at 140 GHz with an FBW of 9 percent, 1.04 dB insertion loss and a return loss of 20 dB.

Through silicon vias (TSVs) replace large interconnects like bond wires or ball grid arrays (BGAs) by allowing vertical routing through the wafer. This makes it possible to stack passive components in three dimensions, integrate them compactly and route signals directly through silicon. A TSV-based tandem cross-coupled SIW bandpass filter with an overall dimension of 0.496 mm × 0.33 mm.[19] It consisted of a top redistribution layer (RDL), a TSV layer and a bottom RDL layer. The top RDL consisted of a feeder, coplanar waveguide slot, S-type slot and remainder RDL layer (the top surface of the six resonator cavities). Based on the tandem cross-coupled topology, TSV positions were set. The bottom layer has an inverted S slot and the feeder. The filter has a center frequency of 0.370 THz with a bandwidth of 0.0165 THz, insertion loss of 2 dB and return loss of 10.7 dB. ***Figure 7*** depicts the TSV-based SIW filter and its response.

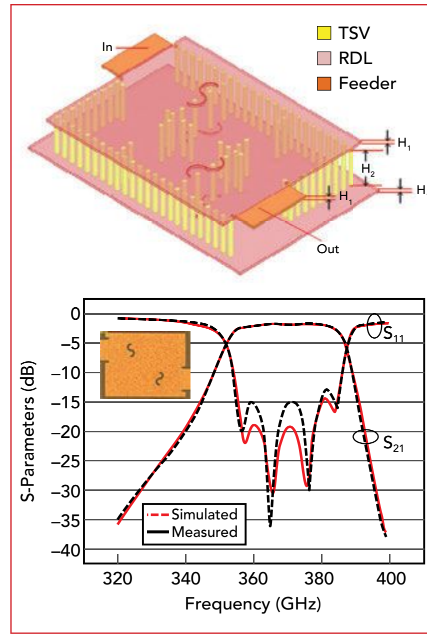

Fig. 7 The TSV-based SIW filter and its response.[19]

Metamaterial-Based Filters

Metamaterial filters are promising candidates for

addressing the challenges of 6G communication, including operation at extremely high frequencies, space constraints and integration with advanced systems such as beamforming antennas and reconfigurable intelligent surfaces (RIS). Metamaterial filters are very compact, possess multiband capability and have high performance, which makes them a plausible choice for 6G communication. Researchers developed a 240 GHz metasurface BPF with a split ring resonator (SRR) matrix.[20] The SRR consisted of two concentric metallic rings with gaps on opposite ends. 30 mm diameter SRR matrices (period 0.8 mm) were fabricated on Rogers Duroid board of 50 μm thickness and copper thickness of 17 μm. They were tested using a Terapulse 4000 system and a 9 mm diameter plane wave, as shown in ***Figure 8***. The filter exhibited an 80 GHz bandwidth and an insertion loss of 0.75 dB. The SRR matrices can be cascaded to improve the filtering response.

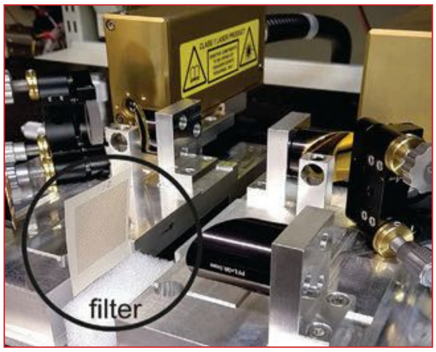

▲ Fig. 8 Filter between beams in a Terapulse 4000 system.[20]

Graphene-Based Filters

Space communication demands robust RF components that can withstand extreme radiation exposure and temperature variations. In deep-space exploration, achieving a high signal-to-noise ratio (SNR) is critical, necessitating low loss and high-selectivity filters. Graphene-based THz filters are promising in this context due to their tunability, radiation hardness and ability to operate efficiently at terahertz frequencies. A graphene-based tunable THz BPF operating at 6.35 THz was developed.[21] The filter consisted of a graphene layer between the conductor and dielectric, facilitating the excitation of surface plasmon modes that enable dynamic frequency tunability. The filter provided precise bandwidth control by adjusting the physical dimensions of the resonator, while the center frequency was tuned by varying the chemical potential of the graphene, achieving a tunable range of approximately 0.16 THz. ***Figure 9*** shows the 3D model of the filter and its response.

CONCLUSION AND FUTURE CHALLENGES

This review summarizes the recent advancements in RF filter technologies for 5G and 6G systems. For 5G, SIW, air-filled SIW, SIGGW and LTCC filters offer compact, low loss and easily integrated solutions. In 6G, advanced materials and structures such as graphene-based filters, SIW extensions and metamaterial-inspired designs like SRRs show potential to meet the demands of higher frequencies and reconfigurability. Moving for-


EXODUS
ADVANCED COMMUNICATIONS
Spotlight on Power
Engineered for Excellence
AMP10134
0.5-26.5 GHz, 1W
AMP10064
20-6000 MHz, 20W
AMP10143
4.0-8.0 GHz, 200W
RF & Microwave Amplifiers
10KHz-75GHz
EMC
MILITARY
COMMERCIAL
AMP20162
10 kHz-250 MHz
2500W
AMP20130
80-1000 MHz
1300W
AMP20184
0.8-2.5 GHz
500W
AMP20160
1.0-6.0 GHz
750W
AMP20178
6.0-18.0 GHz
400W
AMP20167
18.0-40.0 GHz
80W
EXODUS ADVANCED COMMUNICATIONS
www.exoduscomm.com
3674 E. Sunset Road, Suite 100, Las Vegas, Nevada 89120 Tel: 1-702-534-6564

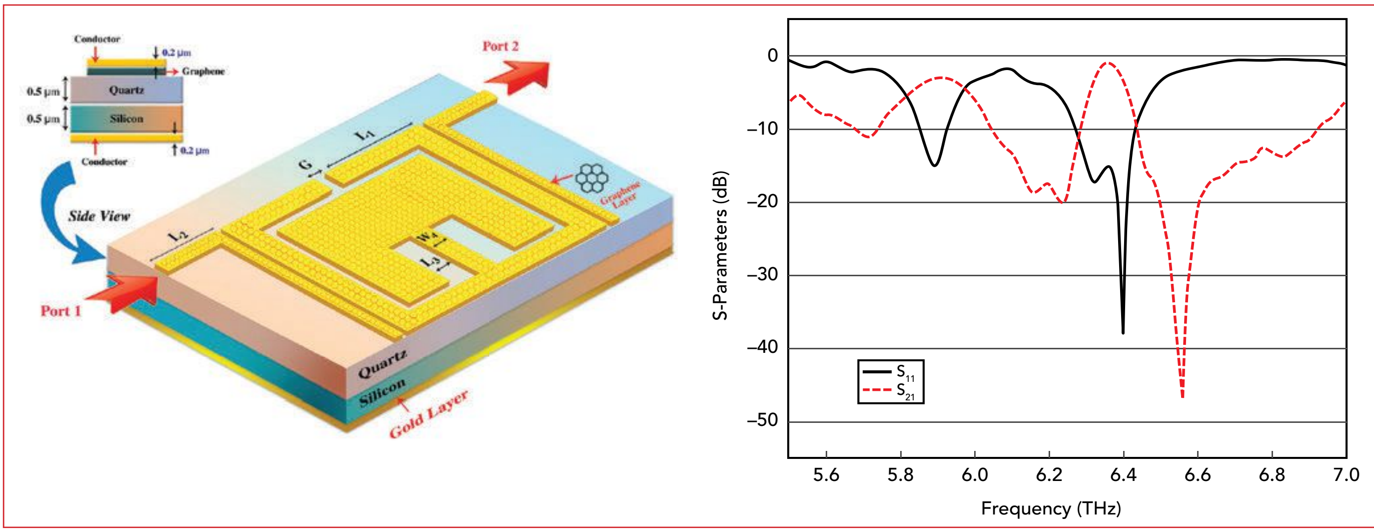

Fig. 9 **Graphene-based THz filter and its response.**[21]

ward, key focus areas include overcoming fabrication and thermal challenges, enhancing tunability and developing hybrid, multifunctional filters. Innovations in AI-assisted design, system-level integration and advanced packaging will be essential to realize high performance, scalable filters for future communication networks.

References:

1. Business Research Insights, "5G mmWave Filters Market Size, Share, Growth, And Industry Analysis, By Type (LTCC 5G mmWave Filters & SAW 5G mmWave Filters), By Application (5G mmWave Smart Phone & 5G mmWave Base Station), Regional Insights and Forecast From 2025 To 2034," Available: https://www.businessresearchinsights.com/market-reports/5g-mmwave-filters-market-105244.
2. Rogers Corporation, "RT/duroid® 5880 Data Sheet," [Online]. Available: https://rogerscorp.com.
3. Murata Manufacturing Co., "LCP and Ceramic Substrates for RF Applications," [Online]. Available: https://www.murata.com.
4. B. Razavi, "Design Considerations for Millimeter-Wave CMOS Radios," *IEEE Journal of Solid-State Circuits,* Vol. 42, No. 5, May 2007, pp. 956–966.
5. R. Camacho-Galeano, R. A. York and A. Oliner, "Loss Mechanisms in High-Q Planar Resonators for RF and Microwave Applications,"

RF-LAMBDA

MADE IN USA

THE LEADER OF RF BROADBAND SOLUTIONS

EMC Broadband RF Power Amplifier

High Power Solid State

HUNDREDS IN STOCK

FAST SHIPPING

FREQUENCY UP TO 90GHZ

POWER UP TO 2KW CW

BENCHTOP AND RACKMOUNT

REMC06G18GG 6-18GHZ 400W

- AUTOMATIC BUILT IN SELF CALIBRATION AND BIAS ADJUSTMENT.
- OVER TEMPERATURE, CURRENT, INPUT POWER PROTECTION.
- VSWR MEASUREMENT AND OPEN CIRCUIT PROTECTION.
- USER FRIENDLY CONTROL INTERFACE.
- REMOTE ETHERNET CONTROL AND FIRMWARE UPDATE.
- HIGH POWER EFFICIENCY AND LIGHTWEIGHT.

RAMP42G47GA 42-47GHZ 8W

REMC02G06GE 2-6GHZ 500W

RAMP18G40GB-U 18-40G 20W

RAMP05M80GC 0.5-80GHZ

REMC18G40GQ 18-40GHZ 200W CW

IEEE Transactions on Microwave Theory and Techniques, Vol. 53, No. 1, January 2005, pp. 38–47.
6. A. Natarajan et al., "A Fully-Integrated 16-Element Phased Array Receiver in SiGe BiCMOS for 60-GHz Communications," *IEEE J. Solid-State Circuits*, Vol. 46, No. 5, May 2011, pp. 1059–1075.
7. Y. Wang et al., "Antenna-Filter Integration for Millimeter-Wave Systems: Techniques and Challenges," *IEEE Access*, Vol. 7, 2019, pp. 186629–186643.
8. S. Pinel et al., "A 60 GHz SoP Integrated Antenna-Receiver Module for High-Speed Wireless Links," *IEEE Trans. Adv. Packag.*, Vol. 27, No. 2, May 2004, pp. 332–338.
9. K. Grenier et al., "Thermal Management in Millimeter-Wave Systems-on-Package," *Microwave Journal*, Vol. 59, No. 10, October 2016, pp. 100–110.
10. L. Ma, J. Zhuang and J. Zhou, "A Cross-coupled Substrate Integrated Waveguide Filter for 28 GHz millimeter wave Communications," *2016 IEEE International Symposium on Circuits and Systems (ISCAS)*, Montreal, QC, Canada, 2016, pp. 814-817, doi: 10.1109/ISCAS.2016.7527365.
11. J.-M. Huang et al., "Substrate-integrated Waveguide Bandpass Filter for 5G Applications," Sensors and Materials, Vol. 36, No. 3, (2024), March 2024, pp. 1105–1113.
12. N. H. Nguyen, F. Parment, A. Ghiotto, K. Wu and T. P. Vuong, "A fifth-order Air-filled SIW Filter for Future 5G Applications," 2017 IEEE MTT-S International Microwave Workshop Series on Advanced Materials and Processes for RF and THz Applications (IMWS-AMP), Pavia, Italy, 2017, pp. 1-3, doi: 10.1109/IMWS-AMP.2017.8247355.
13. Y. Li, C. Tian, S. Li, P. Chen, Y. Li and K. Yang, "Air-filled Substrate Integrated Waveguide Bandpass Filter based on Miniaturized Non-resonant Node Structure," *Int. J. Microw. Wirel. Technol.*, Vol. 16, No. 6, 2024, pp. 919-924, doi: 10.1017/S1759078724000084.
14. C. Segura-Gómez, A. Biedma-Pérez, D. Santiago, Á. Palomares-Caballero, I. Arregui, M. A. Gómez Laso and P. Padilla, "Cavity-stacked Filter in CLAF-SIW Technology for millimeter waves," *AEU - Int. J. Electron. Commun.*, Vol. 193, 2025, p. 155725, [Online]. Available: https://doi.org/10.1016/j.aeue.2025.155725.
15. K. Salehian and M. Tayarani, "A Novel SIGGW Dual Post Bandpass Filter for 5G millimeter-wave Band Applications with a Transmission Zero," *Sci. Rep.*, Vol. 13, article 20743, 2023, doi: 10.1038/s41598-023-47490-1.
16. P. Qiu, Y. Zhang and B. Yan, "A Novel millimeter-wave Substrate Integrated Waveguide (SIW) Filter Buried in LTCC," 2008 Asia-Pacific Microwave Conference, Hong Kong, China, 2008, pp. 1-4, doi: 10.1109/APMC.2008.4958217.
17. X. Zhang, J. Yan, H. Zhang and Y. Chen, "Miniaturized Substrate Integrated Waveguide 5G LTCC Bandpass Filter Exploiting Capacitive Loaded Cavities," *Int. J. RF Microw. Comput.-Aided Eng.*, Vol. 29, No. 11, p. e21730, November 2019, doi: 10.1002/mmce.21730.
18. Z. Luo and K. Zhou, "A D-Band Substrate Integrated Waveguide Bandpass Filter Based on Silicon Carbide Technology," 2023 IEEE MTT-S International Microwave Workshop Series on Advanced Materials and Processes for RF and THz Applications (IMWS-AMP), Chengdu, China, 2023, pp. 1-3, doi: 10.1109/IMWS-AMP57814.2023.10381150.
19. F. Wang, Y. Lu, X. Yin, J. Liu, N. Yu, and Y. Yang, "Miniaturized Silicon-based Substrate Integrated Waveguide Filter for 6G Applications," *Microelectronics Journal*, Vol. 138, 2023, p. 105837, doi: 10.1016/j.mejo.2023.105837.
20. S. Myllymäki and M. Kokkonen, "240 GHz Meta-surface Bandpass Filter and Lens Integration in 6G Telecommunication Systems," *Microw. Opt. Technol. Lett.*, Vol. 63, 2021, pp. 2013–2017, doi: 10.1002/mop.32502.
21. G. C. Ram, N. K. Maurya, S. Yuvaraj, K. B. Sindhuri, D. R. Varma, D. G. Kumar, K. P. Vasavi and S. H. Rao, "Graphene based THz Filter Design using Open-loop Resonator for Space Applications," *Diamond Relat. Mater.*, Vol. 151, 2025, p. 111820, doi: 10.1016/j.diamond.2024.111820.

RF Amplifiers and Sub-Assemblies for Every Application

Delivery from Stock to 2 Weeks ARO from the catalog or built to your specifications!

- Competitive Pricing & Fast Delivery
- Military Reliability & Qualification
- Various Options: Temperature Compensation, Input Limiter Protection, Detectors/TTL & More
- Unconditionally Stable (100% tested)

ISO 9001:2000 and AS9100B CERTIFIED

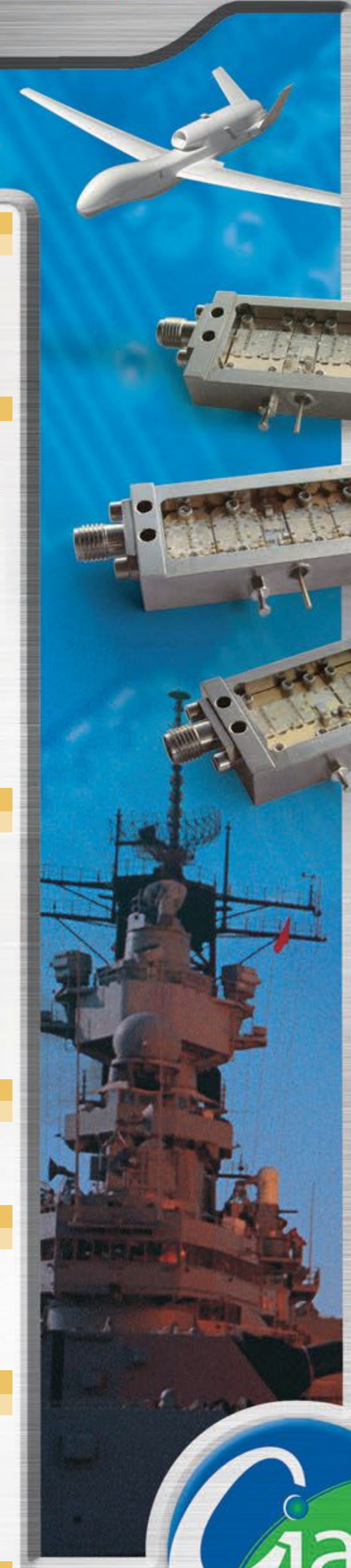

OCTAVE BAND LOW NOISE AMPLIFIERS

Model No.	Freq (GHz)	Gain (dB) MIN	Noise Figure (dB)	Power-out @ P1-dB	3rd Order ICP	VSWR
CA01-2110	0.5-1.0	28	1.0 MAX, 0.7 TYP	+10 MIN	+20 dBm	2.0:1
CA12-2110	1.0-2.0	30	1.0 MAX, 0.7 TYP	+10 MIN	+20 dBm	2.0:1
CA24-2111	2.0-4.0	29	1.1 MAX, 0.95 TYP	+10 MIN	+20 dBm	2.0:1
CA48-2111	4.0-8.0	29	1.3 MAX, 1.0 TYP	+10 MIN	+20 dBm	2.0:1
CA812-3111	8.0-12.0	27	1.6 MAX, 1.4 TYP	+10 MIN	+20 dBm	2.0:1
CA1218-4111	12.0-18.0	25	1.9 MAX, 1.7 TYP	+10 MIN	+20 dBm	2.0:1
CA1826-2110	18.0-26.5	32	3.0 MAX, 2.5 TYP	+10 MIN	+20 dBm	2.0:1

NARROW BAND LOW NOISE AND MEDIUM POWER AMPLIFIERS

Model No.	Freq (GHz)	Gain (dB) MIN	Noise Figure (dB)	Power-out @ P1-dB	3rd Order ICP	VSWR
CA01-2111	0.4 - 0.5	28	0.6 MAX, 0.4 TYP	+10 MIN	+20 dBm	2.0:1
CA01-2113	0.8 - 1.0	28	0.6 MAX, 0.4 TYP	+10 MIN	+20 dBm	2.0:1
CA12-3117	1.2 - 1.6	25	0.6 MAX, 0.4 TYP	+10 MIN	+20 dBm	2.0:1
CA23-3111	2.2 - 2.4	30	0.6 MAX, 0.45 TYP	+10 MIN	+20 dBm	2.0:1
CA23-3116	2.7 - 2.9	29	0.7 MAX, 0.5 TYP	+10 MIN	+20 dBm	2.0:1
CA34-2110	3.7 - 4.2	28	1.0 MAX, 0.5 TYP	+10 MIN	+20 dBm	2.0:1
CA56-3110	5.4 - 5.9	40	1.0 MAX, 0.5 TYP	+10 MIN	+20 dBm	2.0:1
CA78-4110	7.25 - 7.75	32	1.2 MAX, 1.0 TYP	+10 MIN	+20 dBm	2.0:1
CA910-3110	9.0 - 10.6	25	1.4 MAX, 1.2 TYP	+10 MIN	+20 dBm	2.0:1
CA1315-3110	13.75 - 15.4	25	1.6 MAX, 1.4 TYP	+10 MIN	+20 dBm	2.0:1
CA12-3114	1.35 - 1.85	30	4.0 MAX, 3.0 TYP	+33 MIN	+41 dBm	2.0:1
CA34-6116	3.1 - 3.5	40	4.5 MAX, 3.5 TYP	+35 MIN	+43 dBm	2.0:1
CA56-5114	5.9 - 6.4	30	5.0 MAX, 4.0 TYP	+30 MIN	+40 dBm	2.0:1
CA812-6115	8.0 - 12.0	30	4.5 MAX, 3.5 TYP	+30 MIN	+40 dBm	2.0:1
CA812-6116	8.0 - 12.0	30	5.0 MAX, 4.0 TYP	+33 MIN	+41 dBm	2.0:1
CA1213-7110	12.2 - 13.25	28	6.0 MAX, 5.5 TYP	+33 MIN	+42 dBm	2.0:1
CA1415-7110	14.0 - 15.0	30	5.0 MAX, 4.0 TYP	+30 MIN	+40 dBm	2.0:1
CA1722-4110	17.0 - 22.0	25	3.5 MAX, 2.8 TYP	+21 MIN	+31 dBm	2.0:1

ULTRA-BROADBAND & MULTI-OCTAVE BAND AMPLIFIERS

Model No.	Freq (GHz)	Gain (dB) MIN	Noise Figure (dB)	Power-out @ P1-dB	3rd Order ICP	VSWR
CA0102-3111	0.1-2.0	28	1.6 Max, 1.2 TYP	+10 MIN	+20 dBm	2.0:1
CA0106-3111	0.1-6.0	28	1.9 Max, 1.5 TYP	+10 MIN	+20 dBm	2.0:1
CA0108-3110	0.1-8.0	26	2.2 Max, 1.8 TYP	+10 MIN	+20 dBm	2.0:1
CA0108-4112	0.1-8.0	32	3.0 MAX, 1.8 TYP	+22 MIN	+32 dBm	2.0:1
CA02-3112	0.5-2.0	36	4.5 MAX, 2.5 TYP	+30 MIN	+40 dBm	2.0:1
CA26-3110	2.0-6.0	26	2.0 MAX, 1.5 TYP	+10 MIN	+20 dBm	2.0:1
CA26-4114	2.0-6.0	22	5.0 MAX, 3.5 TYP	+30 MIN	+40 dBm	2.0:1
CA618-4112	6.0-18.0	25	5.0 MAX, 3.5 TYP	+23 MIN	+33 dBm	2.0:1
CA618-6114	6.0-18.0	35	5.0 MAX, 3.5 TYP	+30 MIN	+40 dBm	2.0:1
CA218-4116	2.0-18.0	30	3.5 MAX, 2.8 TYP	+10 MIN	+20 dBm	2.0:1
CA218-4110	2.0-18.0	30	5.0 MAX, 3.5 TYP	+20 MIN	+30 dBm	2.0:1
CA218-4112	2.0-18.0	29	5.0 MAX, 3.5 TYP	+24 MIN	+34 dBm	2.0:1

LIMITING AMPLIFIERS

Model No.	Freq (GHz)	Input Dynamic Range	Output Power Range Psat	Power Flatness dB	VSWR
CLA24-4001	2.0 - 4.0	-28 to +10 dBm	+7 to +11 dBm	+/- 1.5 MAX	2.0:1
CLA26-8001	2.0 - 6.0	-50 to +20 dBm	+14 to +18 dBm	+/- 1.5 MAX	2.0:1
CLA712-5001	7.0 - 12.4	-21 to +10 dBm	+14 to +19 dBm	+/- 1.5 MAX	2.0:1
CLA618-1201	6.0 - 18.0	-50 to +20 dBm	+14 to +19 dBm	+/- 1.5 MAX	2.0:1

AMPLIFIERS WITH INTEGRATED GAIN ATTENUATION

Model No.	Freq (GHz)	Gain (dB) MIN	Noise Figure (dB)	Power-out @ P1-dB	Gain Attenuation Range	VSWR
CA001-2511A	0.025-0.150	21	5.0 MAX, 3.5 TYP	+12 MIN	30 dB MIN	2.0:1
CA05-3110A	0.5-5.5	23	2.5 MAX, 1.5 TYP	+18 MIN	20 dB MIN	2.0:1
CA56-3110A	5.85-6.425	28	2.5 MAX, 1.5 TYP	+16 MIN	22 dB MIN	1.8:1
CA612-4110A	6.0-12.0	24	2.5 MAX, 1.5 TYP	+12 MIN	15 dB MIN	1.9:1
CA1315-4110A	13.75-15.4	25	2.2 MAX, 1.6 TYP	+16 MIN	20 dB MIN	1.8:1
CA1518-4110A	15.0-18.0	30	3.0 MAX, 2.0 TYP	+18 MIN	20 dB MIN	1.85:1

LOW FREQUENCY AMPLIFIERS

Model No.	Freq (GHz)	Gain (dB) MIN	Noise Figure dB	Power-out @ P1-dB	3rd Order ICP	VSWR
CA001-2110	0.01-0.10	18	4.0 MAX, 2.2 TYP	+10 MIN	+20 dBm	2.0:1
CA001-2211	0.04-0.15	24	3.5 MAX, 2.2 TYP	+13 MIN	+23 dBm	2.0:1
CA001-2215	0.04-0.15	23	4.0 MAX, 2.2 TYP	+23 MIN	+33 dBm	2.0:1
CA001-3113	0.01-1.0	28	4.0 MAX, 2.8 TYP	+17 MIN	+27 dBm	2.0:1
CA002-3114	0.01-2.0	27	4.0 MAX, 2.8 TYP	+20 MIN	+30 dBm	2.0:1
CA003-3116	0.01-3.0	18	4.0 MAX, 2.8 TYP	+25 MIN	+35 dBm	2.0:1
CA004-3112	0.01-4.0	32	4.0 MAX, 2.8 TYP	+15 MIN	+25 dBm	2.0:1

CIAO Wireless can easily modify any of its standard models to meet your "exact" requirements at the Catalog Pricing.

Visit our web site at www.ciaowireless.com for our complete product offering.

Ciao wireless

Ciao Wireless, Inc. 4000 Via Pescador, Camarillo, CA 93012

Tel (805) 389-3224 Fax (805) 389-3629 sales@ciaowireless.com

NGC Integrates Multiple Antennas to Track Satellites in 1st-Time USSF DARC Demo

Northrop Grumman Corp. and U.S. Space Force (USSF) Space Systems Command's Deep-Space Advanced Radar Capability (DARC) successfully combined the capability of multiple ground-based antennas at DARC Site 1 in Western Australia, demonstrating technology that will create the world's most capable deep-space tracking radar system.

DARC's calibrated antenna arrays operated as a single system to successfully characterize the movement of multiple satellites and demonstrate the effectiveness of the system's precision radar tracking technology. This is a significant step forward as the system progresses toward Site 1's completion and operational capability.

During its demonstration, DARC successfully:

- Used seven of the 27 antennas at DARC Site 1, bringing the program a significant step closer to full capability.
- Demonstrated mission-enabling technology capable of tracking spacecraft that present potential threats to space assets or the U.S. homeland and allies.
- Sustained a multi-week campaign of data collection, analysis and adjustment to confirm successful calibration and operational capability.

DARC is a partnership between the United States, the United Kingdom and Australia, designed to create an all-weather, global system to track very small objects in geosynchronous orbit (GEO) to protect critical U.S. and allied satellite services. Once complete, DARC will track the movement of objects in, to and from GEO with the highest precision, an effective and critical capability for threat detection and mitigation. By leveraging a unique design consisting of multiple ground-based antennas operating together as one, DARC provides unmatched capabilities to enable the USSF's Space Domain Awareness mission.

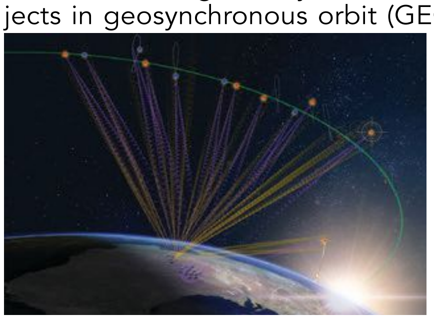

DARC (Source: Northrop Grumman Corporation)

According to Kevin Giammo, director, Space Surveillance and Environmental Intelligence, Northrop Grumman: "Northrop Grumman's DARC will provide a strategic advantage at a scale never before achieved in global space domain awareness. Its ability to track multiple small moving objects over 22,000 miles above earth will offer unmatched persistent and comprehensive capability as the world's premier deep-space radar tracking system."

DARC is a next-generation ground system enabling security and stability in deep space on a global scale. It is specially designed to be the world's most advanced radar for tracking and characterizing objects in deep space. Once complete, DARC's ground-based sensor network will provide full global coverage protecting U.S. and allied satellites in geostationary orbit, a critical area of space traditionally used by some of the most important military and commercial satellites. Unlike telescopic systems which perform this mission today, DARC is not impacted by clouds and can operate 24/7 during nighttime and daylight hours and all-weather conditions.

RTX's LTAMDS Showcases 360-Degree Protection in Latest Test

Raytheon, an RTX business, successfully completed another 360-degree flight test for the Lower Tier Air and Missile Defense Sensor, or LTAMDS, using one of the radar's secondary arrays to track and intercept a complex, threat representative target. This follows the radar's recent Milestone C designation, initiating the transition from prototype to production and deployment.

In this test, LTAMDS, supported an Integrated Battle Command System and a PAC-3 MSE missile intercept of a threat representative target. The test objective was to demonstrate LTAMDS' successful integration with the recently delivered Large Tactical Power Source (LTPS). The increased power provided by LTPS enables LTAMDS to reach its full battlespace potential.

The high capacity, full coverage provided by LTAMDS three radar arrays enable the defeat of massive, coordinated attacks that include a mix of threats such as drones, advanced aircraft, as well as ballistic, cruise and hypersonic missiles. LTAMDS has now completed nine successful flight tests of increasing complexity to prove its capabilities against real-world threats.

"LTAMDS' 360-degree full-sector sensing capabilities specifically address massive, coordinated attacks from adversaries," said Tom Laliberty, president of Land & Air Defense Systems at Raytheon. "As international demand grows, Raytheon continues to invest in our production capacity to quickly deliver this critical capability to customers."

In April 2025, the U.S. Army designated LTAMDS as an official program of record. In 2024 Poland became the first international customer to add LTAMDS to their air and missile defense architecture. Several more countries are actively planning to acquire LTAMDS to modernize their air defenses.

For More Information Visit mwjournal.com for more defense news.

DARPA Christens Unmanned Ship Aimed at Revolutionizing Naval Capability

DARPA recently marked a traditional naval milestone with the christening of USX-1 Defiant, a first-of-its-kind autonomous, unmanned surface vessel designed from the ground up to never accommodate a human aboard. The ceremony took place at Everett Ship Repair in Everett, Washington.

The demonstrator for the No-Manning-Required Ship (NOMARS) program, the Defiant, has a simplified hull design to enable rapid production and maintenance in nearly any port facility or Tier III shipyard that traditionally supports yacht, tug and workboat customers.

The 180 foot-long, 240-metric-ton lightship is completing final systems testing in preparation for an extended at-sea demonstration of reliability and endurance.

"Defiant is a tough little ship and defies the idea that we cannot make a ship that can operate in the challenging environment of the open ocean without people to operate her," said NOMARS Program Manager Greg Avicola, during the ceremony. "While relatively small, Defiant is designed for extended voyages in the open ocean, can handle operations in sea state 5 with no degradation and survive much higher seas, continuing operations once the storm passes. She's no wider than she must be to fit the largest piece of hardware and we have no human passageways to worry about."

The NOMARS program leapfrogs conventional thinking about unmanned ships, with a goal to minimize the need for "optionally manned" vessels and safely demonstrate the reliability and capability of fully unmanned systems to strengthen the nation's defense industrial base.

"Defiant class vessels provide cost-effective, survivable, manufacturable, maintainable, long-range, autonomous and distributed platforms, which will create future naval lethality, sensing, and logistics," said DARPA Director Stephen Winchell. "Defiant will protect and expand the capabilities of manned ships, multiply combat power at low cost, and unlock new American maritime industrial capacity."

After completing the at-sea demonstration, Defiant will be turned over to the U.S. Navy's Unmanned Maritime Systems Program Office (PMS 406). DARPA is working closely with the Navy to identify a pathway to ensure capabilities and technologies demonstrated throughout the NOMARS program are accessible for rapid transition and integration, are scalable and support international defense partnerships.


Reactel, Inc.
Reacting First to All Your Filter Needs.
Filter Solutions For Mission Critical Applications
High Performance, Rugged Packaging, Small Size and Weight
Great things can come in small packages. Reactel filters are ideally suited for the demanding environments that unmanned vehicles encounter.
Many manufacturers rely on Reactel to provide units which are:
High performance - Lightweight - Low profile
Contact a Reactel engineer with your filter or multiplexer requirements. We can create a unit which will be the perfect fit for your applications.
REACTEL, INC.
RF & Microwave Filters - Multiplexers - Multifunction Assemblies
REACTEL, INC.
REACTEL, INC.
REACTEL, INC.
8031 Cessna Avenue • Gaithersburg, Maryland 20879 • (301) 519-3660 • reactel@reactel.com • reactel.com
Intertek
RoHS
MADE IN MD
Since 1979

ATIS Next G Alliance Advances Industry Understanding of Joint/Integrated Communication and Sensing for 6G Innovation

The Alliance for Telecommunications Industry Solutions (ATIS)' Next G Alliance (NGA) announced the publication of "Channel Measurements and Modeling for Joint/Integrated Communication and Sensing, as well as 7–24 GHz Communication Channels, Phase II."

Spectrum spanning 7 to 24 GHz, particularly the 7 to 15 GHz segment, is poised to play a pivotal role in next-generation wireless, starting with 6G features. Among the six key usage scenarios identified for this band is Joint/Integrated Communication and Sensing (J/ICAS), which reuses existing telecommunications infrastructure for RF sensing with no need for active transmissions from objects being detected.

The Phase II white paper builds upon the foundational measurements and models presented in the NGA's July 2024 Phase I report on the topic. Phase I delivered initial channel modeling for both midband (7 to 24 GHz) and mmWave frequencies; Phase II extends the work by:

- Conducting additional measurements of communication channels across the 7 to 24 GHz range.
- Introducing enhanced sensing channel models that account for both target reflections and environmental interactions.
- Focusing on, among other areas, sensing background characterization in urban street canyon environments and providing a more rigorous sensing background channel model that captures the non-sparsity of clutter echoes.

"The advanced research effort that went into this paper represents one of the industry's most comprehensive studies of integrated communication and sensing capabilities for future wireless systems," said Jaydee Griffith, managing director of the NGA. "It is another contribution that highlights the NGA's position as the industry leader driving the innovation behind 6G development."

"The Next G Alliance Technology & Roadmap Working Group (TRWG) has been actively advancing the understanding of 6G channel characteristics in both midband (7 to 15 GHz) and 28 GHz frequencies, with a focus on communication and Integrated Sensing and Communication (ISAC) applications," said Amitava Ghosh (Nokia), chair of the NGA TRWG.

"This Phase II report delivers valuable new insights into a range of communication environments and includes updated penetration loss measurements at midband frequencies, as well as detailed radar cross-section and background characterizations essential for ISAC," Ghosh continued.

Glass in Semiconductors: The Next Inflection in Semiconductors

Glass in semiconductors is not a moon-shot concept; it already sits quietly inside modern fab. Ultra-flat borosilicate carriers hold silicon wafers during backside thinning, sodium-free sheets form hermetic MEMS caps, and low-coefficient of thermal expansion (CTE) glass is the baseplate for many wafer-level fan-out processes.

Glass is gradually moving from a background consumable to the heart of a package, providing the core substrate, the interposer that links chiplets, and the dielectric that shapes sub-THz signals or steers photons on their way to optical fiber.

IDTechEx has released a new market report, "Glass in Semiconductors 2026-2036: Applications, Emerging Technologies, and Market Insights," providing end-to-end market intelligence for seven distinct glass product segments, with technology deep-dives, benchmarking, supply chain mapping, adoption drivers, risk analysis and unit and revenue forecasts 2025-2036.

The catalyst in the shift for glass is the escalating bandwidth and power density of AI and high-performance computing devices. A single training accelerator already requires thousands of high-speed I/O bumps and a power-delivery network that handles hundreds of amps with minimal noise. Organic-based laminate, the workhorse of the last twenty years, struggles to maintain the required flatness and via density in response to ever-increasing demand. Silicon interposers offer far finer wiring, but at a price and panel size that limited applications cannot justify.

Glass slides neatly between these extremes. Its CTE can be tailored to match silicon; its loss tangent is an order of magnitude lower than silicon at 40 GHz, and large-panel processing potential from the LCD industry means a single sheet can be half a meter on one side at costs that trend toward high-end organics as yields rise.

The surging demand for AI and high-performance computing is forcing every layer of the packaging stack to carry more current, more I/O, and higher signaling speeds than organic laminates or even first-generation silicon interposers can comfortably support. These pressures have turned glass core substrates and large-panel glass interposers from a niche curiosity into commercialization.

Leading device makers and materials vendors are now openly investigating the technology: Intel has demonstrated glass-based test vehicles on its Arizona path-finding line, Samsung Electronics is exploring glass cores as a potential option alongside its I-Cube and H-Cube packages, substrate major SKC has installed a pilot drill-and-fill line for 500 mm glass panels and glass giant AGC is supplying low-CTE borosilicate sheets for early evaluations.

For More Information Visit mwjournal.com for more commercial market news.

No company has yet nailed down a production launch date, but the collective effort signals a clear shift; glass is firmly on the shortlist of next-generation substrate candidates for the AI/HPC era. The trend is reflected by the emergence of glass core substrate and interposers, especially for advanced packaging and IC substrates.

High-frequency and photonic integration widen the addressable market. Glass's low dielectric loss and optical transparency give it a second growth engine beyond compute packaging. At Ka-band and above, insertion loss through glass microstrip is roughly half that of an equivalent organic line.

Photonics adds still another pull. Co-packaged optics aims to move fiber attach from the front panel of a switch to the substrate that sits millimeters from the switch ASIC. Engineered glass can carry both the electrical redistribution layers and the low-loss waveguides, simplifying alignment and eliminating costly silicon photonic interposers. Because the same through-glass via (TGV) technology used for RF can create vertical optical vias, a single core can support trans-impedance amplifiers, laser drivers and the optical waveguide itself. This convergence of electronic and photonic routing plays directly to glass's strengths and pushes its potential market beyond conventional electronics packaging.

Glass's march from pilot lines to volume hinges less on raw material availability – melting furnaces exist in every region – than on the emerging ecosystem of laser drilling, copper filling, panel handling and design automation. Yield learning curves, via-fill reliability, panel warpage and design-kit maturity will determine whether glass meets the cost targets set by system integrators. Understanding who is installing capacity, which drilling techniques are moving from proof-of-concept to 24/7 production, and how quickly design tools can model gigahertz losses or sub-micron warpage is therefore essential for anyone betting on the timing of adoption.

Equally important is the competitive dynamic with silicon and improved organics. Foundries are pushing hybrid wafer-level redistribution that narrows the feature-size advantage glass holds, while laminate suppliers are developing next-generation Ajinomoto Build-up Film (ABF) cores with lower roughness and better CTE matching. The IDTechEx report benchmarks pros and cons across these materials so readers can see clearly where glass is likely to win, and where it will remain a specialty option.

Around the **Circuit**

Barbara Walsh, Multimedia Staff Editor

MERGERS & ACQUISITIONS

CommScope announced it has entered into a definitive agreement to sell its Connectivity and Cable Solutions (CCS) segment to **Amphenol Corp**. for approximately USD $10.5 billion in cash, to be paid by Amphenol upon closing. The sale is expected to close within the first half of 2026, subject to customary closing conditions, including receipt of applicable regulatory approvals and the affirmative vote of the shareholders. The vote is required under Delaware law due to the nature and size of the transaction.

AT&T has agreed to purchase certain wireless spectrum licenses from **EchoStar** for a total of approximately $23 billion in an all-cash transaction, subject to certain adjustments. AT&T and EchoStar have also agreed to enhance their long-term wholesale network services agreement, enabling EchoStar to operate as a hybrid mobile network operator providing wireless service under the Boost Mobile brand. AT&T will be the primary network services partner to EchoStar as it continues to serve wireless customers. AT&T will acquire approximately 30 MHz of nationwide 3.45 GHz mid-band spectrum.

COLLABORATIONS

Rohde & Schwarz has taken a significant step forward in satellite testing technology by delivering a fully customized solution to the **Taiwan Space Agency** (TASA). For the first time, Rohde & Schwarz integrated EMC and antenna measurement capabilities into a single test chamber, addressing a complex challenge in satellite payload testing. The innovative system, now operational at TASA's facility, reflects the growing need for advanced satellite testing methodologies. With the increasing adoption of non-terrestrial network technologies, precise validation of satellite performance in complex environments is becoming essential. This includes ensuring seamless integration between satellites and cellular base stations — an area where conventional testing methods often fall short.

Microwave Vision Group (MVG) and **Anritsu** announce the availability of a joint testing solution supporting over-the-air (OTA) validation of non-terrestrial network (NTN) communications for mobile and IoT devices. MVG has adapted its multi-probe OTA systems to integrate the capabilities of Anritsu's Radio Communication Analyzer MT8821C, delivering a lab-based environment for realistic satellite link emulation in compliance with 3GPP requirements. As NTN deployments gain momentum — particularly through LEO satellite constellations — mobile and IoT devices must now demonstrate robust performance under conditions that differ significantly from terrestrial operation.

Sumitomo Electric Industries, Ltd. and **Osaka Metropolitan University** have successfully fabricated a GaN transistor (GaN-HEMT) on a 2-in. polycrystalline diamond (PCD) substrate in a joint research project with the Japan Science and Technology Agency. This technology is an important step toward achieving higher capacity and lower power consumption of core devices in mobile and satellite communications. In recent years, as the volume of information in wireless communications has increased, there has been a demand for higher frequencies and higher output powers in high-frequency devices such as GaN-HEMTs. However, the self-heating that occurs during operation limits the devices' output power, resulting in signal transmission failures and other problems that reduce the performance and reliability of communications.

Thin Film Interconnect, based in Frederick, Md., announced a strategic technology partnership with **Heisler Semiconductor LLC**, headquartered in Baltimore, Md. This collaboration combines the technical strengths of two Maryland-based innovators to deliver a complete, end-to-end solution for wafer production, through silicon via (TSV) deposition and full turn-key heterogeneous packaging. Beyond technological advancements, TFI and Heisler Semiconductor are actively contributing to workforce development initiatives. Through collaborations with universities and partnerships with startups and defense contractors, the companies are helping train the next generation of semiconductor engineers and providing real-world access to leading-edge fabrication and packaging technologies.

Eridan announced a strategic partnership with **Skylark Wireless** to deliver high performance Open RAN solutions designed to power the next generation of wireless infrastructure. The collaboration is supported by recent NTIA grant awards through the Public Wireless Supply Chain Innovation Fund, part of a federal initiative to accelerate U.S.-based innovation in secure, open wireless networks. Skylark will incorporate Eridan's MIRACLE radio unit into its fully software-defined massive MIMO architecture.

NEW STARTS

Backed by its two Excellence Supplier Awards from **Maxar** in 2023 and 2024, **Anywaves** has already demonstrated its ability to deliver best-in-class products to the American market. The company is taking the next step as it transitions from an international presence to a true multinational organization with the launch of Anywaves US. With the U.S. hosting most of the global space industry's business, being closer to its key American customers and partners will allow Anywaves to refine its product roadmap and ensure even stronger market fit.

EnSilica is establishing of a new design centre in Budapest, Hungary. The facility strengthens EnSilica's presence in the European Union and taps into Budapest's deep technology ecosystem, which hosts numerous leading automotive and industrial multinationals. This expansion will increase the group's global headcount to around 210

For More Information

For up-to-date news briefs, visit mwjournal.com

employees. EnSilica has also announced it has established a new engineering hub in Cambridge, U.K.

ACHIEVEMENTS

Leonardo DRS, Inc. announced that is has successfully completed its first series of open-water demonstrations of its advanced maritime Mission Equipment Package (MEP) for counter UAS (C-UAS) naval fleet protection. The DRS Maritime MEP is a scalable C-UAS system based on DRS's proven land-based mobile short-range air defense and C-UAS systems. This system is designed to be mounted on a range of small uncrewed surface vessels providing remote ship protection at varying distances, providing a real solution as the Navy looks to autonomous surface vessels to protect ships from air and surface threats.

AccelerComm announced that it has closed a funding round totaling $15 million. The capital will be used to further develop and accelerate deployments of the company's 5G satellite communications products and technology that enable direct-to-device (D2D) communications between phone handsets and space-based satellite networks. The round was led by IP Group, including its Parkwalk and Hostplus managed funds, with support from IQ Capital, Swisscom Ventures' digital transformation fund and Bloc Ventures. The investment will support the company's ongoing implementations with key mobile operator and satellite network customers and partners, including Lockheed Martin.

SFL Missions Inc. announced the successful launch and deployment of the GHGSat-C12 and GHGSat-C13 (also known as Pierre and Valmay, respectively) greenhouse gas monitoring microsatellites developed for GHGSat of Montreal. SFL Missions Inc. developed the satellites on a low-cost, high-performance 15-kg NEMO bus, the same used to build the first nine GHGSat spacecraft. GHGSat-C12 and -C13 launched on June 23 from Vandenberg Space Force Base, California, aboard the SpaceX Transporter 14 ride-share mission. Ground control has established communications with both spacecraft. GHGSat is the world leader in emissions monitoring technologies and pioneered the first satellite capable of detecting and measuring facility-level greenhouse gas emissions from space.

CONTRACTS

The **U.S. Army** has awarded **Lockheed Martin** a $720 million contract for the production of Joint Air-to-Ground Missiles (JAGM) and HELLFIRE missiles, marking the fourth and final follow-on award as part of its current multiple-year contract. This contract will provide critical procurement and production support for the U.S. Army, U.S. Navy and international customers, further solidifying Lockheed Martin's position as a leading provider of multi-domain missile systems. Under this contract, Lockheed Martin will deliver JAGM and HELLFIRE missiles to meet the urgent operational needs of the Army, Navy and its international partners. The contract includes key Foreign Military Sales (FMS) including 160 JAGMs for the United Kingdom.

Around the **Circuit**

The Department of Defense (DOD) recently announced that **Raytheon** has been awarded a $258 million contract for the engineering, manufacturing and development of SM-2 Block IIICU All Up Rounds. This is a new contract for the follow-on integration and test phase of a development program Raytheon has been in contract for. The majority of this work will be performed in Tucson, Ariz., and is expected to be completed by September 2031. SM-2 is a cornerstone of a ship's layered defense. It provides firepower against high-speed, highly maneuverable anti-ship missiles and aircraft and protects naval assets that give warfighters greater operational flexibility.

Sidus Space announced the next milestone under its expanded $120 million preliminary agreement with **Lonestar Data Holdings** Inc. to support the world's first lunar data centers. Atomic-6 has been selected to supply its Light Wing™ solar arrays which are expected to power Sidus' LizzieSat® satellites supporting Lonestar's cislunar data storage constellation.

Sivers Semiconductors announced it has received a purchase order from **aiRadar Inc.** The order is for the development of a state-of-the-art 28 GHz antenna module based on Sivers' high performance TRX BF02 beamforming transceiver chip. The new antenna module will power aiRadar's latest radar systems targeting both commercial and defense markets, with an emphasis on defense applications such as high performance drone platforms. The collaboration combines Sivers' expertise in advanced RFIC design with aiRadar's cutting-edge radar technology to deliver a compact, high-resolution radar solution with next-generation capabilities.

PEOPLE


▲ *Duncan Pilgrim*

At **Marki Microwave**, **Duncan Pilgrim** will be stepping into the role of Chief Commercial Officer. Since joining in 2020 as Vice President of Sales and Marketing, Duncan has been critical to the expansion of Marki's global footprint and driving revenue growth. As CCO, he will lead Marki Microwave's next phase of innovation with a continued focus on robust commercial strategy and customer impact. Also Kris Rausch has joined Marki as Vice President of Global Sales, bringing over 30-years of RF industry expertise and a passion for leading dynamic sales teams. He will be instrumental in accelerating Marki's worldwide sales strategy.


▲ *Mark Crebs*

Naprotek, LLC announced the appointment of **Mark Crebs** to Products and Platform Director of Business Development. Mark brings over 25 years of experience in sales and business development, including roles in national and regional sales management and in roles with major electronic components distributors across North America.

Nxbeam

Ku/ Ka/ V/ E-Band Power Amplifier MMICs

Maximized performance for linear power applications

Ku/Ka-Band MMIC Die and Packaged MMICs

MMIC Die:

NPA1020-DE	12.5 - 14.5 GHz	15 W
NPA2020-DE	23.0 - 25.0 GHz	10 W
NPA2001-DE	26.5 - 29.5 GHz	35 W
NPA2002-DE	27.0 - 30.0 GHz	35 W
NPA2003-DE	27.5 - 31.0 GHz	35 W
NPA2004-DE	25.0 - 27.5 GHz	40 W
NPA2030-DE	27.5 - 31.0 GHz	20 W
NPA2040-DE	27.5 - 31.0 GHz	10 W

QFN Packaged MMICs:

NPQ2101-SM	27.5 - 31.0 GHz	5 W
NPQ2103-SM	27.5 - 31.0 GHz	8 W
NPQ2105-SM	27.5 - 31.0 GHz	12 W
NPQ2107-SM	27.5 - 31.0 GHz	15 W

Contact Nxbeam for Flange Packaged Options

V-Band MMICs

MMIC Die:

NPA4000-DE	47.0 - 52.0 GHz	1.5 W
NPA4010-DE	47.0 - 52.0 GHz	3.0 W

E-Band MMICs

MMIC Die:

NPA7000-DE	65.0 - 76.0 GHz	1.0 W

INVITED PAPER

EMI Shielding: Metal Braids to Next-Generation Composite Solutions

Ralph Schafer
Micro-Coax, an Amphenol Company, Pottstown, Penn.

In the pursuit of higher performance and greater efficiency, modern electronic systems face an increasingly complex challenge: electromagnetic interference (EMI). As devices become more sophisticated and densely packed, the risk of EMI increases. Signal integrity, once a manageable concern, now demands innovative solutions that can keep pace with evolving technology while meeting stringent constraints on weight, flexibility and environmental resilience.

This convergence of challenges has sparked a fundamental re-evaluation of EMI shielding technologies, driving engineers to seek solutions that transcend the limitations of conventional approaches while maintaining superior performance. "We are seeing electromagnetic environments that are orders of magnitude more complex than what we dealt with even a decade ago," says Ralph Schafer, Technical Director, Defense and Aerospace Electronics at Micro-Coax. "The traditional copper braids that served us well in legacy systems simply cannot keep up with the performance demands of modern avionics while meeting our weight and flexibility requirements." However, advancements in materials science have led to the development of high performance alternatives that are quickly reimagining the future of EMI shielding.

UNDERSTANDING TRADITIONAL METAL BRAIDS

For decades, copper and tinned copper braids have served as the backbone of EMI shielding solutions across countless applications. Their widespread adoption stems from a combination of electrical conductivity, mechanical strength and cost-effectiveness that has made them the frequent choice for engineers worldwide.

Traditional metal braids function by creating a conductive pathway that intercepts electromagnetic fields and redirects them to ground, effectively creating a Faraday cage around sensitive conductors. The interwoven structure provides multiple current paths, ensuring redundancy and maintaining shielding effectiveness even when individual strands fail. This redundancy, combined with the conductivity of copper, has made metal braids particularly effective at lower frequencies.

The manufacturing processes for copper braids are well-established and widely available, contributing to their cost-effectiveness and reliable supply chain. Standard braiding equipment can produce consistent, high-quality shields with predictable electrical and mechanical properties. Additionally, installation procedures are straightforward, requiring only basic tools and techniques.

However, the very properties that made copper braids successful in earlier generations of technology now present significant limitations in modern applications. The density of copper, approximately 8.96 grams per cubic centimeter, becomes a critical constraint when system designers face strict weight budgets. Mechanical properties present another challenge, as copper braids exhibit "mechanical memory," a tendency to retain shape after bending that can create stress concentrations in underlying conductors. This rigidity not only restricts design flexibility but can also shorten a system's lifespan in dynamic environments.

MODERN EMI ENVIRONMENTS

Today's electromagnetic environment presents challenges that extend beyond the capabilities for which traditional shielding was initially designed. The proliferation of electronic systems operating at higher frequencies has created a complex interference landscape where multiple signals compete for spectrum space within increasingly compact packages. This complex electromagnetic environment leads to a host of problems, including signal degradation, data corruption and, in some cases, system failure. Moreover, the push for smaller, lighter and more powerful electronics means that devices are often packed closer together, exacerbating the potential for crosstalk

RELIABLE ELECTRONIC SOLUTIONS

iNRCORE®
FAMILY OF BRANDS

INDUSTRIES SERVED

SPACE

DEFENSE/MILITARY

COMMERCIAL AEROSPACE

MEDICAL

POWER & DISTRIBUTION

TRANSPORTATION

SIGNAL
Ethernet, Transceiver Modules, MIL-STD-1553, Data Bus Couplers, Baluns, Delay Lines

FILTERS
Bandpass, High Pass, Low Pass, Band Reject, Notch, EMI/RFI, Bias Tee, Amplitude Equalizer, Diplexers / Multiplexers

TRANSFORMERS
Flyback, Buck/Boost, Isolation, Current Sense, Impedance, SMT, THT, MIL-STD-981, MIL-PRF-27

CAPACITORS
High-Q/Low ESR Multi-Layer Ceramic, Broadband, Single Layer, Thin Film, Variable

RESISTORS
Wirewound, Surge, Thin/Thick Film, Carbon Composition, Ressitor Arrays, High Power, Edge Wound Tubular, Metal Film, Microwave

INDUCTORS
Power, RF, High Frequency, High Q, Military QPL, Planar, Conical, Ceramic Chip, Toroidal, CMC, THT, SMT, MIL-STD-981, MIL-PRF-27

SUPPORTING YOUR COMPLETE PRECISION ELECTRONIC COMPONENT NEEDS

For more info
SCAN HERE!
www.inrcore.com/brands/

and unwanted electromagnetic coupling.

High frequency applications reveal fundamental limitations in traditional metal braids. As frequency increases, the skin effect becomes more pronounced, confining current flow to the surface of conductors. The braided structure itself can create apertures that allow high frequency energy to penetrate the shield, a phenomenon known as "windowing" that becomes more problematic as operating frequencies climb into the GHz range.

Weight constraints in commercial and defense aerospace applications have intensified. "In commercial aviation, we are literally counting grams," notes Schafer. "When you multiply a few hundred grams of weight savings per harness across an entire aircraft, you are looking at significant fuel savings over the aircraft's operational lifetime. The environmental and economic benefits are impossible to ignore."

WHERE TRADITIONAL SOLUTIONS FALL SHORT

Engineering analysis reveals several critical areas where traditional metal braids struggle to meet modern performance requirements. Flexibility represents the most significant limitation, particularly in applications requiring frequent movement or tight packaging constraints. Because copper is a soft metal, thicker strands are required for strength in a standard copper braid. The necessary thickness adds weight to the braid and reduces its flexibility.

Installation complexity adds another layer of difficulty. Traditional metal braids require specialized tools for cutting and termination, and their inherent stiffness can complicate routing through tight spaces or around complex geometries. The "mechanical memory" of copper braids means they retain bending stress, potentially creating strain on delicate cable assemblies.

DRIVING PROGRESS WITH NEW MATERIALS

The limitations of traditional metal braids have driven intensive research into advanced materials that can deliver superior EMI shielding while addressing weight, flexibility and environmental challenges. "The breakthrough came when we realized we did not need solid metal throughout the entire cross-section," says Schafer. "By applying conductive coatings to high-strength polymer fibers, we could achieve the electrical performance of metals while maintaining the flexibility and weight advantages of textiles."

Aramid fibers, particularly DuPont™ Kevlar®, have emerged as promising base materials for next-generation shielding solutions. These synthetic polymers offer exceptional strength-to-weight ratios, approximately five times stronger than steel by weight, while maintaining flexibility and resistance to environmental degradation. The fibrous structure of aramids provides an ideal substrate for metallic coatings that can deliver the conductivity required for EMI shielding.

Metal plating technologies have evolved to enable the deposition of conductive layers on polymer substrates. Silver and nickel coatings can be applied to

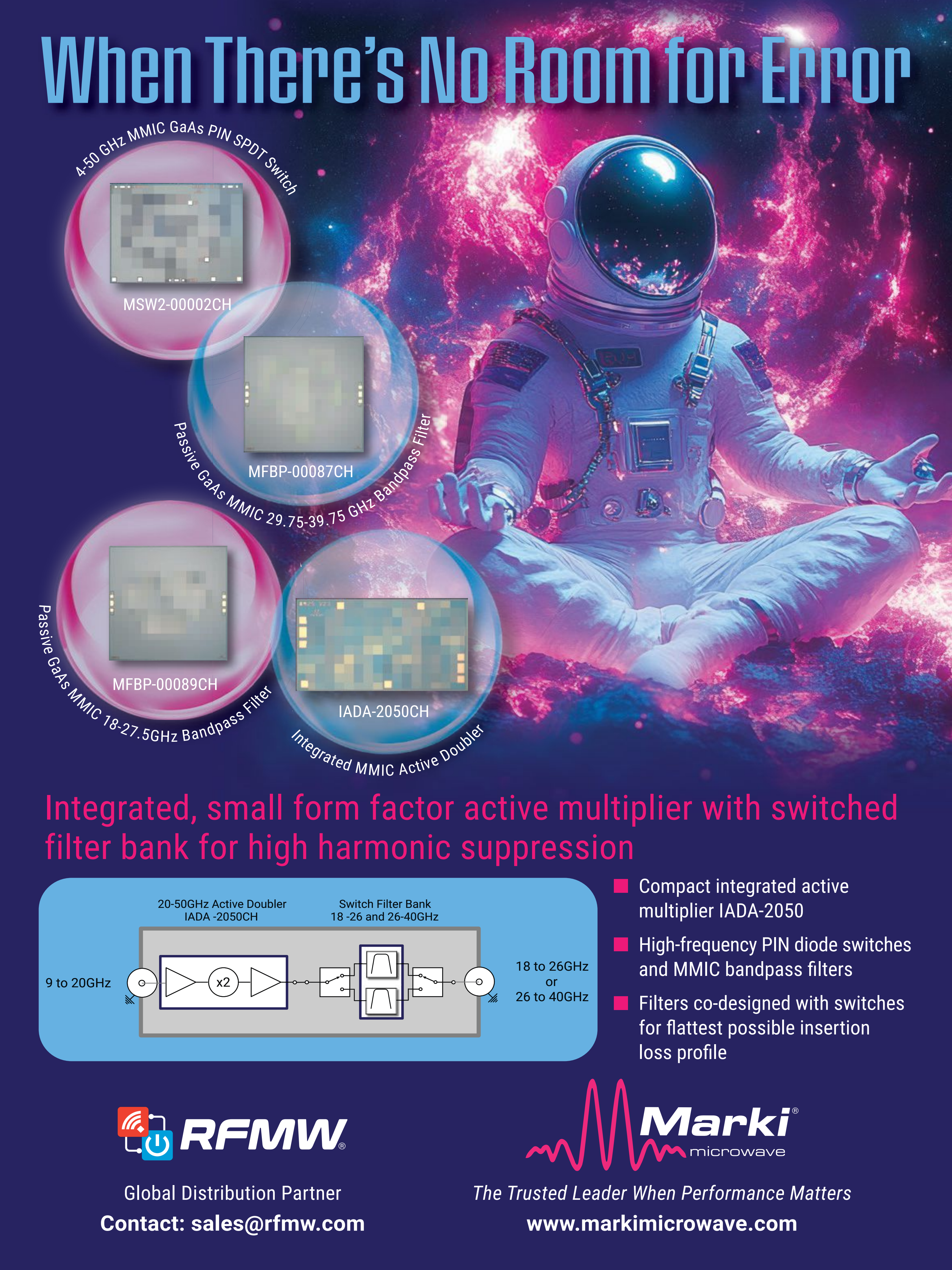

When There's No Room for Error
4-50 GHz MMIC GaAs PIN SPDT Switch
MSW2-00002CH
Passive GaAs MMIC 29.75-39.75 GHz Bandpass Filter
MFBP-00087CH
Passive GaAs MMIC 18-27.5GHz Bandpass Filter
MFBP-00089CH
Integrated MMIC Active Doubler
IADA-2050CH
Integrated, small form factor active multiplier with switched filter bank for high harmonic suppression
20-50GHz Active Doubler
IADA -2050CH
Switch Filter Bank
18 -26 and 26-40GHz
9 to 20GHz
x2
18 to 26GHz
or
26 to 40GHz
Compact integrated active multiplier IADA-2050
High-frequency PIN diode switches and MMIC bandpass filters
Filters co-designed with switches for flattest possible insertion loss profile
RFMW®
Global Distribution Partner
Contact: sales@rfmw.com
Marki® microwave
The Trusted Leader When Performance Matters
www.markimicrowave.com

aramid fibers through various processes, creating composite materials that combine the lightweight, flexible properties of the polymer core with the electrical conductivity of the metallic coating.

The ultra-fine filament structure achievable with advanced composite materials offers significant advantages for EMI shielding applications. Finer filaments can be packed more densely, increasing the surface area available for improving shielding effectiveness at high frequencies. The increased surface-to-volume ratio enhances the skin effect benefits while maintaining structural integrity.

ENVIRONMENTAL AND OPERATIONAL ADVANTAGES

Advanced composite shielding materials offer significant advantages in environmental resistance and operational performance. The polymer core provides inherent resistance to corrosion, eliminating many of the degradation mechanisms that affect traditional metal braids. This resistance is particularly valuable in naval applications, where salt spray and humidity create hostile environments for conventional metals.

Temperature performance represents another area where composite materials excel. While copper braids can experience significant expansion and contraction with temperature changes, composite materials maintain more stable dimensions across temperature ranges. This stability is crucial in aerospace applications where systems may experience temperature excursions from -110°C to +150°C or higher.

Fig. 1 Artist's rendition of a satellite.

The outgassing characteristics of advanced composite materials make them suitable for space applications (see ***Figure 1***), where vacuum conditions can cause traditional materials to release gases that contaminate sensitive optical systems. Materials engineered to meet ASTM E-595 requirements for low outgassing can maintain their properties in the vacuum environment of space while avoiding contamination issues.

MEETING MODERN DEMANDS FOR EMI SHIELDING

Looking ahead, the evolution of EMI shielding technology appears poised to continue along multiple parallel paths. Materials science

Fig. 2 ARACON cable from Micro-Coax.

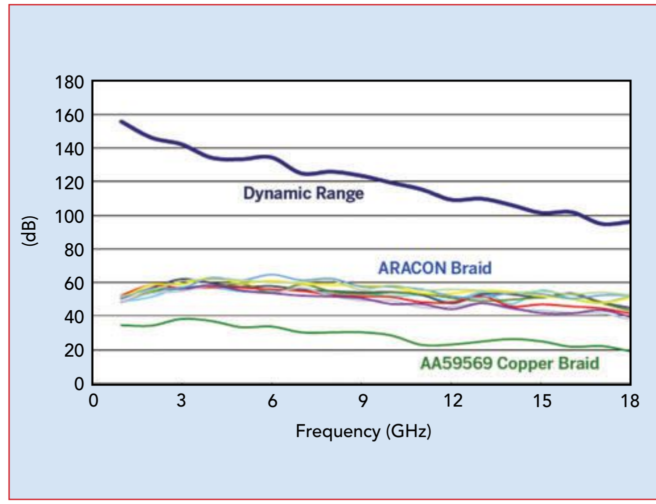

Fig. 3 **Shielding data for ARACON versus copper braids.**

advances will yield new composite materials with even better performance characteristics. Manufacturing technology will continue to evolve, potentially enabling the production of custom-engineered shielding materials optimized for specific applications. Additive manufacturing techniques may allow for the creation of complex three-dimensional shielding structures that would be impossible to achieve using traditional braiding techniques.

The integration of smart materials and sensing capabilities into EMI shielding represents another frontier for innovation. Shielding materials that can monitor their own performance, detect damage or adapt to changing electromagnetic environments could revolutionize how we approach EMI management in critical systems.

THE FUTURE OF EMI SHIELDING

The transition from traditional metal braids to advanced composite shielding materials marks a fundamental evolution in EMI management. While copper braids remain cost-effective for legacy systems, the demanding requirements of aerospace, defense and advanced electronics necessitate materials that transcend conventional limitations.

Metal-clad aramid fiber systems like ARACON® fiber from Micro-Coax, as shown in ***Figure 2***, deliver the electrical performance of copper with improvements in weight, flex life and environmental resistance, as demonstrated in ***Figure 3***. These materials transform system design by eliminating the trade-offs between EMI shielding effectiveness and mechanical performance that have constrained engineers for decades.

As electromagnetic environments increase in complexity, advanced composite shielding materials provide the performance characteristics essential for next-generation systems, enabling design innovations previously impossible with traditional approaches. ■

Kevlar® is a registered trademark of DuPont. DuPont™ is a trademark of DuPont.

ARACON® is a registered trademark of Amphenol CIT.

INVITED PAPER

Power Dividers Versus Power Splitters

Jason Yoho, Ameya Ramadurgakar and Madrone Coopwood
HYPERLABS, Louisville, Colo.

While the terms "power divider" and "power splitter" are often used interchangeably, there is a fundamental difference in their designs and intended applications. Power dividers (2-way) typically utilize a three-resistor configuration and are used for dividing a single input signal into multiple output signals for applications such as signal distribution. Power splitters, often employing a two-resistor configuration, are primarily used for leveling and ratio measurements. Both power dividers and power splitters can function as power combiners.

POWER DIVIDERS

A three-resistor RF power divider, shown in ***Figure 1***, is a passive circuit that produces a 1:2 split of an incoming RF signal into two output signals. The design typically uses three resistors having a value of 16.6 Ω, often in a star or tee configuration, to divide the power while maintaining a consistent impedance match and signal integrity across a wide frequency range, assuming all ports are terminated in 50 Ω. These dividers are known for their simplicity and wide bandwidth, but they also introduce insertion loss due to the resistive nature of the circuit. Assuming all outputs are terminated into 50 Ω, the RF power divider presents a 50 Ω load to a signal source connected at Port 1 (input). In this case, the device transmits one quarter of the input power, or -6 dB, to Port 2 and Port 3. 3 dB of the loss is generated from the power dividing, and 3 dB of the loss is generated in the resistors.

These devices can be manufactured in several ways, including a series of surface-mount thin film or thick film resistors on a printed circuit board or a series of thin film resistors made of tantalum nitride (TaN) or nichrome (NiCr) on a ceramic substrate. TaN resistors are very stable and reliable after they are passivated at high temperatures, whereas NiCr resistors are used in specialty applications where a low temperature coefficient of resistance (TCR) is required.[2] The power handling capability of the circuit is mainly based on the size of the resistors and the ability of the device to either control or disperse the heat generated from the resistive loss.

Power dividers are usually specified by the power handling and bandwidth of the circuit and the

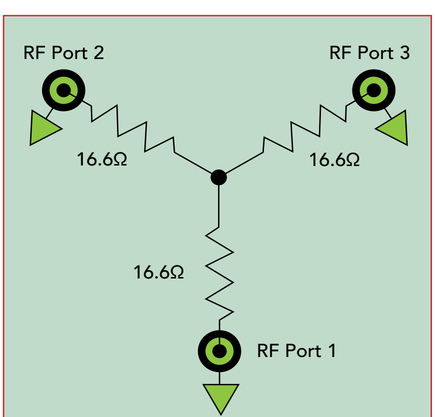

Fig. 1 **1:2 three-resistor power divider schematic.**

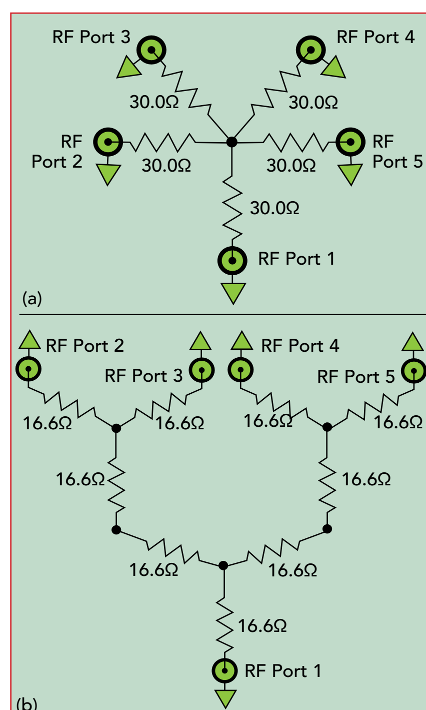

Fig. 2 **1:4 power divider schematic a) in a star pattern and b) as concatenated 1:2 power dividers.**

amplitude and phase balance of the two output ports relative to the input port. Since the circuit is a resistive, passive design, it functions from DC to the maximum cutoff frequency of the design. There are currently offerings on the market with bandwidths specified from DC to greater than 110 GHz.

Power dividers can be designed to have more than two outputs by concatenating multiple 1:2 power dividers or by using a greater number of resistors sharing a common node. ***Figure 2*** shows two examples of manufacturing a 1:4 power divider. ***Figure 2a*** incorporates five 30 Ω resistors in a star pattern. This methodology has some drawbacks in dividing the power of the input signals equally among the remaining four ports due to the physical symmetry of the design. At high frequencies, more energy enters the ports opposite the input than enters the adjacent ports.

A more common implementation is to use three 1:2 power dividers, shown in Figure 1, resulting in the schematic shown in ***Figure 2b***. This topology ensures equal power division, each -12 dB down from the input signal, and an identical group delay across the four outputs. The main drawback to the topology shown in Figure 2b is that the power divider has a dedicated input port, and the isolation between each of the output ports is not identical.

The final power divider for discussion is one that creates an unequal power division between the two outputs. ***Figure 3*** shows a topology where all the ports are matched to 50 Ω, but the power delivered to Port 2 and Port 3 is unequal. This component is more commonly referred to as a resistive coupler or an impedance-matched pick-off tee. A common (unequal) divider ratio would select the four resistors to supply -4 dB to Port 2 while supplying -10 dB to Port 3 (both relative to Port 1), while keeping all three ports matched to 50 Ω.

POWER SPLITTERS

A two-resistor RF power splitter, shown in ***Figure 4***, is a passive circuit that produces a 1:2 split of an incoming RF signal into two output signals. This design typically utilizes

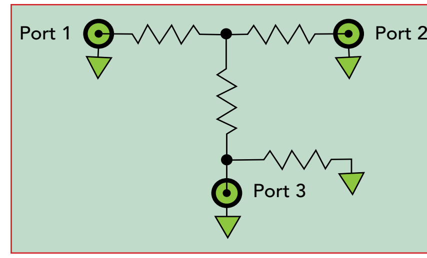

Fig. 3 Unequal power divider schematic.

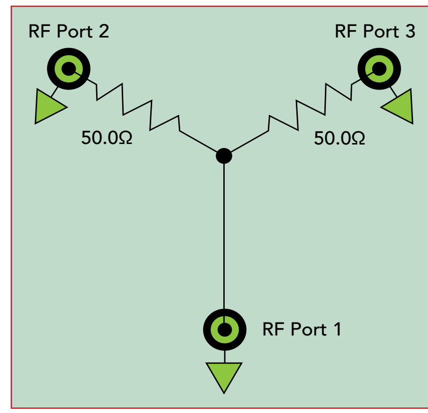

Fig. 4 1:2 two-resistor power splitter.

two resistors, each having a value of 50 Ω. A power splitter is a simple and common method to split power in RF circuits, particularly in applications like gain measurements and leveling loops.

The input impedance at Port 1 is matched to 50 Ω when the outputs, Port 2 and Port 3, are terminated in 50 Ω. In contrast, the outputs of the resistive power splitter look like 83.3 Ω when all ports are terminated to 50 Ω.

The unique feature of a power splitter is best defined when the port impedance on both Port 2 and Port 3 is not 50 Ω and/or unequal. In this case, the power splitter delivers equal incident power to both loads irrespective of the load imbalance. Since equal incident power is constant regardless of load impedance imbalances, the two-resistor power splitter is used where the ratio of output power to a reference signal is needed. To understand this phenomenon further, one must review 3-port network theory and investigate the scattering parameters (S-parameters) of both the power divider and the power splitter.

3-PORT NETWORK THEORY

To better understand the function of a power divider versus a power


Frontlynk®
Bridging Gaps
Multi Coax
Probe Multi Coax up to 67GHz
RF.Microwave Coaxial Connector
& Cable Assembly
1.0mm Series
Connectors, Adaptors,
and Cable Assemblies
up to 110GHz
1.0mm Connector
DC to 110GHz, VSWR≤1.2
1.35mm Connector
DC to 90GHz, VSWR≤1.2
1.85mm Connector
DC to 67GHz, VSWR≤1.2
2.4mm Connector
DC to 50GHz, VSWR≤1.2
2.92mm Connector
DC to 40GHz, VSWR≤1.15
3.5mm Connector
DC to 34GHz, VSWR≤1.15
1.35mm Series up to 90GHz
Test Cables up to 110GHz
Frontlynk Technologies Inc.
www.frontlynk.com
Tel: +886-6-356-2626
Fax: +886-6-356-6268
E-mail: info@frontlynk.com

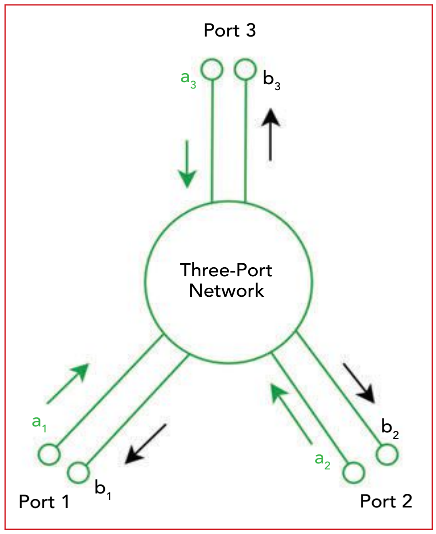

Fig. 5 Three-port device flow diagram.

TABLE 1

S-PARAMETERS OF A RESISTIVE POWER DIVIDER VERSUS A RESISTIVE POWER SPLITTER[1]

	Power Divider	Power Splitter
S_{11}	0	0
S_{12}	0.5	0.5
S_{13}	0.5	0.5
S_{21}	0.5	0.5
S_{22}	0	0.25
S_{23}	0.5	0.25
S_{31}	0.5	0.5
S_{32}	0.5	0.25
S_{33}	0	0.25

splitter, it is helpful to review the S-parameters of 3-port RF devices. A 3-port network can be visualized as shown in ***Figure 5***.

Referring to Figure 5, each port is represented in terms of inward-going (incident) voltage wave "a_n" and outward-going (reflected) voltage wave "b_n." The subscript "n" represents the port number associated with the wave. S-parameters can be used to represent voltage transfer functions within and across ports. By definition, each port that is not being actively stimulated with incident energy is assumed to be terminated with a 50 Ω load. For example, S_{11} is the ratio of the reflected "b" wave at Port 1 (b_1) to the incident "a" wave at Port 1 (a_1) with no signal applied at the other two ports.

$$S_{11} = \frac{b_1}{a_1} \mid a_2 = a_3 = 0 \qquad (1)$$

Similarly, S_{21} is the ratio of the outward-going "b" wave at Port 2 (b_2) to the incident "a" wave at Port 1 (a_1) with no signal applied at the other two ports.

$$S_{21} = \frac{b_2}{a_1} \mid a_2 = a_3 = 0 \qquad (2)$$

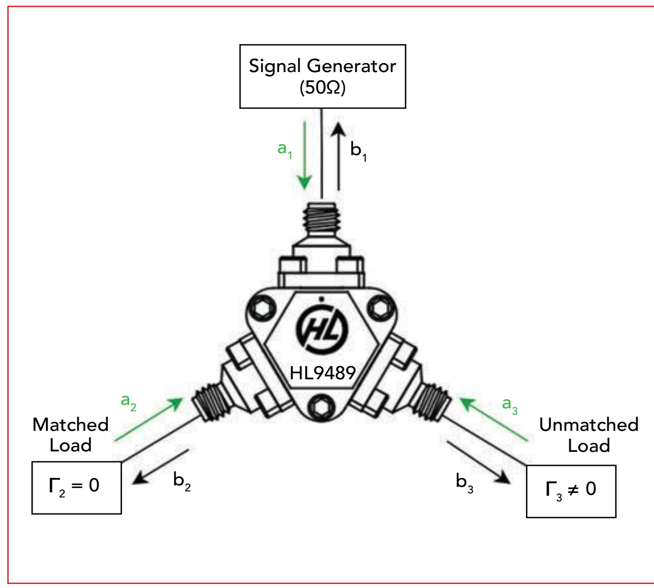

Fig. 6 Power splitter example with an unmatched load.

A full linear matrix shown in Equation 3 can be used to describe the incident and reflected wave relations of a 3-port device as follows.

$$\begin{pmatrix} b_1 \\ b_2 \\ b_3 \end{pmatrix} = \begin{pmatrix} S_{11} & S_{12} & S_{13} \\ S_{21} & S_{22} & S_{23} \\ S_{31} & S_{32} & S_{33} \end{pmatrix} \begin{pmatrix} a_1 \\ a_2 \\ a_3 \end{pmatrix} \qquad (3)$$

S-PARAMETERS OF POWER DIVIDERS AND SPLITTERS

The fundamental differences between three-resistor power dividers and two-resistor power splitters are well understood and documented in literature.[1] The work by B. Smith presents the differences between the two components and derives the scattering parameters of both devices.[1] These results are best summarized in ***Table 1***.

The three-resistor power di-

MiCable

0.6~7.25GHz

High Accuracy Butler Matrices

NEW

ONE MODEL COVER **5G NR(FR1) / WiFi 6E** Freq. Bands

Excellent Phase Accuracy & Amplitude Unbalance

Low VSWR / Low I.L. / High Isolation

Good Stability & Repeatability

P / N	Structure	Freq. Range (GHz)	VSWR Max. (:1)	Insertion Loss* Max. (dB)	Amplitude Unbal. Max. (dB)	Amplitude Flatness Max. (dB)	Phase Accuracy Max. (Deg.)	Isolation Min. (dB)
SA-07-4B006073	4x4	0.617-0.96	1.4	8.2	±1.1	±0.8	±11	17
		1.427-2.69	1.5	8.7	±1	±1	±10	14
		3.3-5	1.5	9.2	±1	±1	±12	14
		5.15-7.25	1.6	9.8	±1.1	±1.1	±12	13
SA-07-8B006073	8x8	0.617-0.96	1.4	12	±1.5	±1.4	±13	17
		1.427-2.69	1.5	13.2	±1.4	±1.6	±12	14
		3.3-5	1.5	14.6	±1.4	±1.6	±14	14
		5.15-7.25	1.6	15.9	±1.5	±1.7	±14	13

*Theoretical Insertion Loss Included

— Typical Test Curve** —

SA-07-4B006073

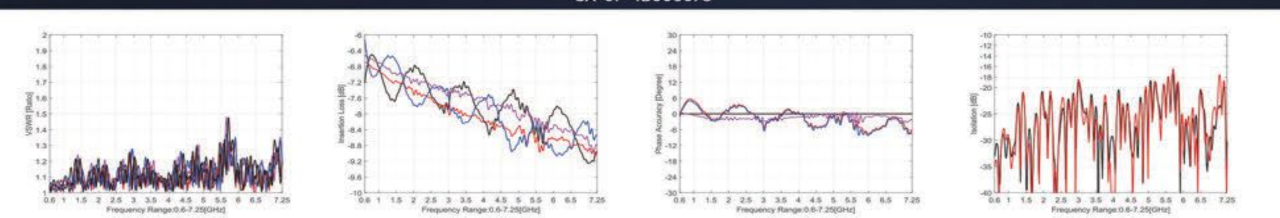

**Corresponding Channels: A1B1、A1B2、A1B3、A1B4

More Information-
Scan the QR Code

MIcable Inc.

www.micable.cn sales@micable.cn +86-591-87382856

vider has an impedance match, resulting in no reflections on all ports ($S_{11}=S_{22}=S_{33}=0$) and 6 dB of isolation between output ports ($S_{23}=S_{32}=0.5$). In contrast, the power splitter has 12 dB return loss on the output ports ($S_{22}=S_{33}=0.25$) and 12 dB of isolation between output ports ($S_{23}=S_{32}=0.25$). This gives the power splitter a distinct advantage when driving imbalanced loads. If energy is reflected from an unmatched load and arrives back at the output of the power splitter, one quarter of that energy is re-reflected, and one quarter is transmitted to the opposite output. "This maintains an equal power output from the two ports".[1] This scenario is illustrated in ***Figure 6***.

The parameters in Equations 3 and 4 become apparent when inspecting the forward and reflected waves.

$$S_{23} = \frac{b_2}{a_3} \tag{4}$$

$$S_{33} = \frac{b_3}{a_3} \tag{5}$$

Using the data in Table 1, one can now see the advantages of a power splitter by looking at the expressions in Equations 6 and 7. The equations show that the energy reflected from the unmatched load on Port 3 is equally re-reflected to both Port 2 and Port 3, keeping the ratio of the two outputs at a constant.

$$b_2 = 0.25a_3 \tag{6}$$

$$b_3 = 0.25a_3 \tag{7}$$

POWER SPLITTER – APPLICATION

One application for a power splitter is a ratio measurement, as shown in ***Figure 7***. This setup will provide a ratio of the transmitted signal through the device under test (DUT) relative to the detected signal on the second power splitter output. This measurement will result in the gain of the DUT.

The previous S-parameter calculations demonstrate that both outputs of the power splitter are identical ($S_{21} = S_{31}$) and that the reflections from the DUT are equally split to both outputs of the device. With this knowledge, it is assured that only the gain of the DUT is being measured, regardless of the imped-

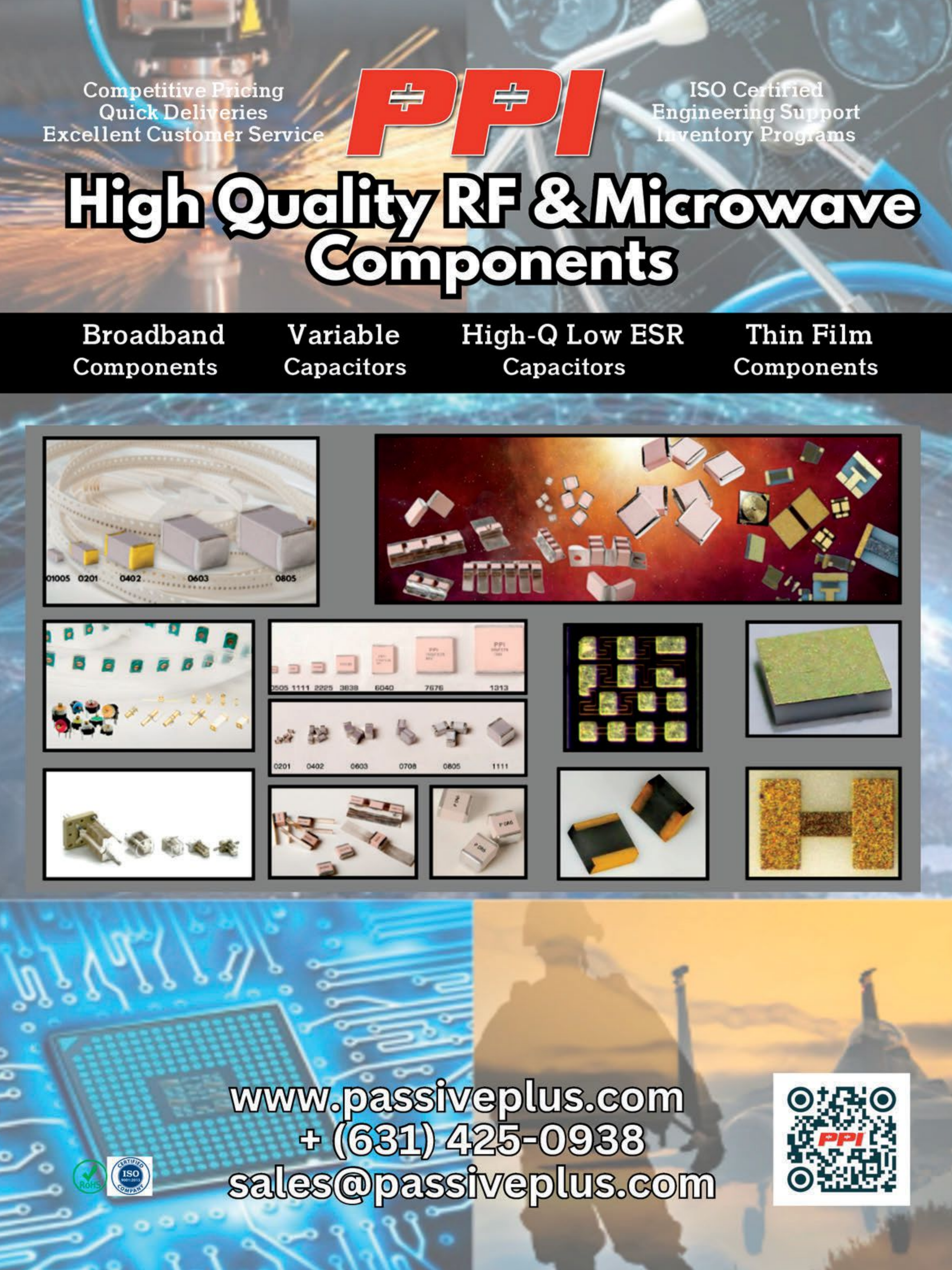
Competitive Pricing
Quick Deliveries
Excellent Customer Service
PPI
ISO Certified
Engineering Support
Inventory Programs
High Quality RF & Microwave Components
Broadband Components
Variable Capacitors
High-Q Low ESR Capacitors
Thin Film Components
01005 0201 0402 0603 0805
0505 1111 2225 3838 6040 7676 1313
0201 0402 0603 0708 0805 1111
www.passiveplus.com
+ (631) 425-0938
sales@passiveplus.com

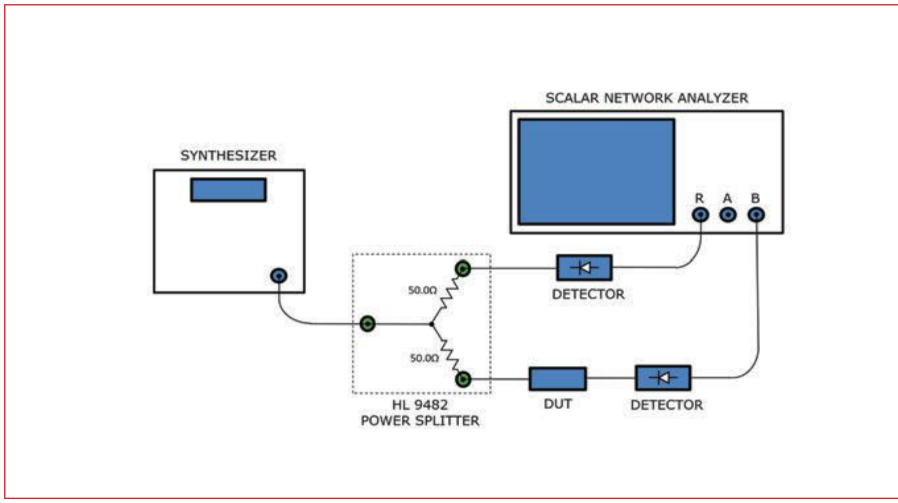

Fig. 7 Ratio DUT transmission measurement using a power splitter.

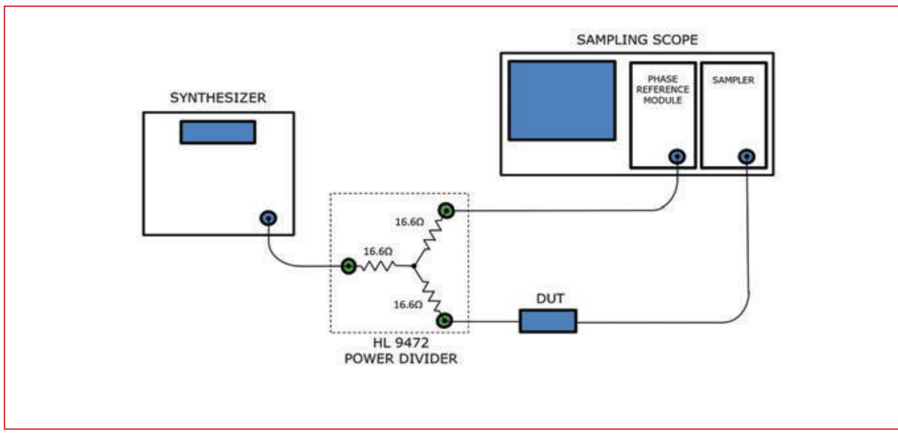

Fig. 8 Power divider used as a clock fanout.

ance seen by the output of the power splitter that is driving the DUT.

POWER DIVIDER - APPLICATION

A standard application for a power divider, shown in ***Figure 8***, is to use it for clock signal distribution. In this application, the power divider is being driven with a clock signal generated by an RF synthesizer. Once the clock signal is divided into two identical signals, one signal can be used to drive the DUT, and the other can be used to drive the phase reference module of the equivalent-time sampling scope.

In any application where a clock signal needs to be duplicated, a power divider will create two or more in-phase versions of the clock source.

CONCLUSION

Power dividers and power splitters are both devices that divide/split an input signal into multiple output signals, but they differ in their design and intended use. Three-resistor power dividers are designed to distribute power evenly among multiple output ports, while two-resistor power splitters can be designed for various power division ratios and applications.

This article is intended as an introduction to the differences between power dividers and power splitters by presenting the S-parameters that differentiate them from one another. Specific application examples have been provided for each device to help further the understanding of the noted differences. ■

References

1. B. Smith, "Choosing the Right Power Splitter: Two-Resistor or Three-Resistor." Power Splitter vs. Divider, www.dinfo.unifi.it, n.d.
2. "Design Guidelines," UltraSource, [Online]. Available: https://www.yourthinfilmsource.com/design-guidelines/.


GaN

Microwave Assisted Non-Invasive Detection of Adulteration in Milk

Prodyuti Sarkar and Piyali Basak
Jadavpur University, India

Rahul Mondal, Snehasish Saha and Partha Pratim Sarkar
University of Kalyani, India

There are various physical, chemical and biochemical methods of solid or liquid food analysis that have evolved to identify the quality and quantity of contaminants or adulterants (i.e., impurities) in food. Most of those methods, however, are time-consuming, expensive, laborious and difficult to access. They also require expert food analysts. In water and liquid food products, adulterants or contaminants are dissolved and cannot be detected or isolated easily. The experimental procedure demonstrated here seeks to reduce these challenges. It detects food impurities in liquids using microwave radiation by observing changes in the transmission coefficient. In this work, pure double-toned milk is used as the liquid food product under test along with three different types of adulterants (detergent, starch and water). Adulterants blended in concentrations as low as 0.03 percent by weight of fresh milk are effectively measured. The method is low-cost, contactless and scalable.

According to a 2015 World Health Organization (WHO) report on the estimates of the global burden of foodborne diseases, an estimated 600 million, almost 1 in 10 people in the world, fall ill after eating contaminated food, and 420,000 die every year. Children under 5 years of age carry 40 percent of the foodborne disease burden, with 125,000 deaths every year. Therefore, food poisoning and foodborne diseases have a very adverse effect on the society and economy of a nation. The first step to improve this situation is to incorporate proper methods of detecting any impurities in food products before marketing them for sale.

Food products are contaminated voluntarily or involuntarily while undergoing industrial processing, preservation and packaging. To reduce food loss and improve food safety, the food business must detect various types of impurities.[1]

Prior to the marketing and sale of food products in India, samples are tested by food testing laboratories and quality control laboratories established by the Food Safety and Standards Authority of India (FSSAI), as

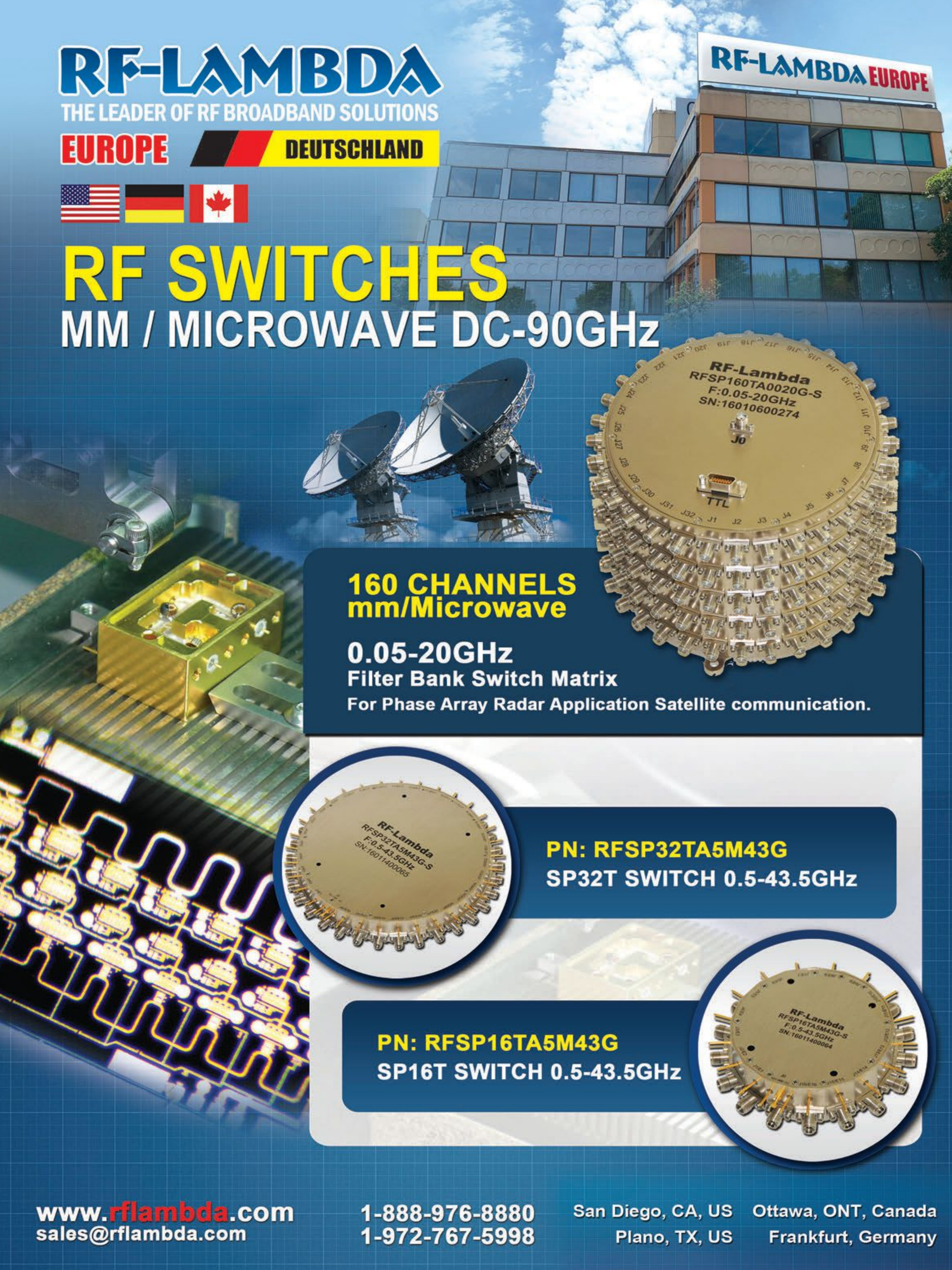
RF-LAMBDA
THE LEADER OF RF BROADBAND SOLUTIONS
EUROPE
DEUTSCHLAND
RF-LAMBDA EUROPE
RF SWITCHES
MM / MICROWAVE DC-90GHz
RF-Lambda
RFSP160TA0020G-S
F:0.05-20GHz
SN:16010600274
160 CHANNELS
mm/Microwave
0.05-20GHz
Filter Bank Switch Matrix
For Phase Array Radar Application Satellite communication.
PN: RFSP32TA5M43G
SP32T SWITCH 0.5-43.5GHz
PN: RFSP16TA5M43G
SP16T SWITCH 0.5-43.5GHz
www.rflambda.com
sales@rflambda.com
1-888-976-8880
1-972-767-5998
San Diego, CA, US
Plano, TX, US
Ottawa, ONT, Canada
Frankfurt, Germany

well as by certain commercial food testing laboratories. To determine the kind and amount of impurity, a variety of physical, chemical and biological methods of analysis have been developed; however, these methods are time-consuming, costly, labor-intensive, difficult to obtain and require skilled food analysts.

Mass spectroscopy, gas chromatography, liquid chromatography, near-infrared (NIR) chromatography, hyper-spectral imaging and X-ray imaging are some of the currently used food testing techniques. These require sophisticated equipment and modern technology. In addition to these methods, several chemical tests on food components are employed to detect foreign substances. There are only a small number of food testing laboratories available in India with these capabilities, and they are limited to areas close to large cities.

This work focuses on the detection of impurities in liquid food products. It is generally easier to identify adulterants in solid food products. In water or liquid food products, impurities dissolve, making them more challenging to isolate and identify.

Measurements are performed using milk as the liquid food product. Milk is a balanced food containing most of the necessary nutrients; it is a staple for children, sick and elderly people. If milk and milk products are contaminated or adulterated, then a considerable percentage of the population is impacted.[1]

Milk is found to be adulterated with detergent, starch and other substances by merchants, wholesalers and retailers for monetary benefit. Additionally, water is intentionally added to increase volume without cost before sale. A national survey on milk adulteration conducted by the FSSAI in 2011 revealed that detergents, skimmed milk powder and impure water are found in about 70 percent of the milk consumed in India, which is similar to other developing nations as well.[2]

One such adulterant is starch, which is usually added to increase the solid non-fat milk content. Excessive amounts of starch in milk remain undigested and are reported to cause threatening diseases like diarrhea.[3,4] Furthermore, high levels of starch accumulated in the body may be fatal for diabetic patients.

Adulterated milk does not provide necessary nutrients and might result in other health issues such as migraines, vision problems, hypertension, kidney stones and even death.[5-7] After the Chinese milk crisis in 2008, in which infant milk products were adulterated with melamine to boost nitrogen content, milk adulteration has been highlighted as a global concern.[8] Therefore, the rapid and accurate identification of adulterants in milk is essential for quality control and food safety assurance.

Generally, mixing impurities in a liquid modifies its dielectric properties. Microwave sensors using split ring resonators (SRRs) and complementary SSR technology have been proposed to measure the concentration of contaminants in fluids by sensing changes in their dielectric properties.[9-14] These techniques, however, demand high-precision sensors and typically require contact with the liquid under test.

Other methods have been explored to determine the percentages of adulterants in milk. Sadat et al.[15] used the electrical conductance of sampled milk, but controlling this condition in the market is difficult. Durante et al.[16] proposed the measurement of the electrical impedance property of sampled milk for real-time detection of bovine milk adulteration. Here, as well, contactless measurement is not possible.

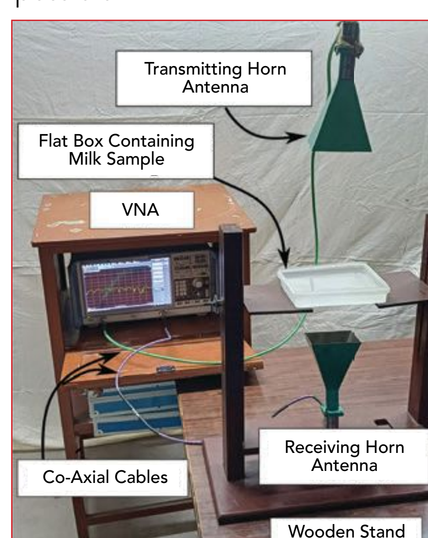

Fig. 1 Test setup.

The experimental procedure described in this work overcomes the challenges of the previously mentioned techniques. It demonstrates the detection of impurities present in liquid food products using microwave radiation. Because the presence of impurities in a liquid food product changes its dielectric properties, the reflection and transmission of incident microwave radiation change as well. Measured data reveal characteristic changes in a liquid's transmission coefficient magnitude ($|S_{21}|$) for specific types of food products and impurities. Moreover, this provides the benefit of being a contactless measurement technique.

METHODOLOGY

This is based on the principle that variations in a material's dielectric constant or relative permittivity measurably influence its transmission characteristics at microwave frequencies. When a microwave signal within a specific frequency band propagates through a material, its transmission depends on the material's dielectric constant.[17] The transmission coefficient (S_{21}) of electromagnetic radiation passing

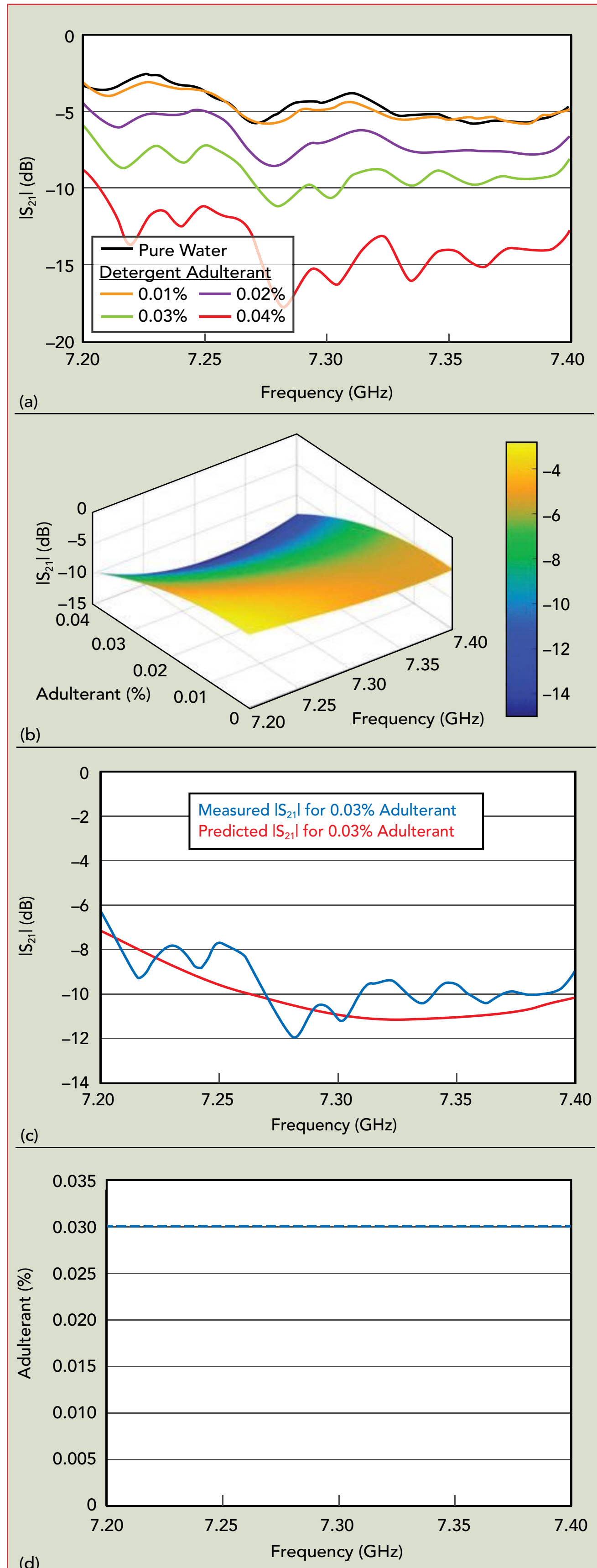

Fig. 2 Measured $|S_{21}|$ of detergent in water (a), predicted $|S_{21}|$ (b), measured and predicted $|S_{21}|$ for 0.03 percent adulterant (c) and predicted concentration for a given $|S_{21}|$ (d).

through two materials (in this case, air and liquid) is governed by ***Equation 1:***

$$S_{11} = \frac{2\eta_2}{\eta_1 + \eta_2} \quad (1)$$

where, η_1 and η_2 are the intrinsic impedances of the air and liquid media, respectively.

The intrinsic impedance of a medium is given by ***Equation 2***:

$$\eta = \sqrt{\frac{\mu}{\varepsilon}} \quad (2)$$

where μ is the permeability and ε_r is the permittivity ($\varepsilon = \varepsilon_o\, \varepsilon_r$) of the medium.

As ε_r in the liquid increases, η_2 decreases, which in turn reduces $|S_{21}|$. According to Maxwell's equations and Fresnel's transmission theory, $|S_{21}|$ is inversely related to the dielectric constant of the medium. As permittivity increases, the intrinsic impedance (η_2) of adulterated milk decreases, leading to a higher absorption of incident microwave radiation. Adulterants, such as water, starch or detergent added to pure milk alter its dielectric properties by increasing ε_r. The increase in each case is monotonic with the increased percentage of adulterant.[18] Therefore, adulterants in milk result in decreased microwave signal transmission, which is measurable.

In this work, pure double-toned milk from Anand Milk Union Limited (AMUL) is the material under test and different types of adulterants are added in separate experiments. Each of the materials under test has a distinctly different dielectric constant. When compared to pure milk, the reflection and transmission characteristics of the adulterated milk are different as well. Based on this principle, pure double-toned milk is distinguished from the adulterated forms.

MEASUREMENT SETUP AND PROOF OF CONCEPT

The measurement setup is shown in ***Figure 1***. A thin, flat plastic 25 cm × 16 cm × 3.3 cm^3 container containing the liquid under test is suspended between two 8 to 12 GHz horn antennas. $|S_{21}|$ is measured with a Rohde and Schwarz ZNB 20 VNA. Note that these measurements are performed without the use of an anechoic chamber in an uncontrolled environment. The goal of this work is to demonstrate the ability to measure the percentage of adulterants or contaminants in a location outside of a laboratory where the surroundings are uncontrolled or natural. A handheld VNA and X-band horn antennas are portable. They can be easily carried and set up in any location. This may result in some variability in the data over frequency, which can be fit to a smooth curve, as shown in ***Figure 2***.

Prior to the measurements of adulterants in milk, an experimental trial is carried out using distilled water as the solvent and detergent as the adulterant. Detergent powder having a weight/volume ratio (weight of detergent/volume of water) from 0.01 to 0.04 percent is added consecutively to the distilled water. $|S_{21}|$ is measured for the different detergent concentrations. For these measurements, the depth of the sample liquid is 1 cm.

Measured $|S_{21}|$ of detergent as an adulterant in pure water versus frequency is plotted in ***Figure 2a***. Using the sample data points of transmission coefficients, $|S_{21}|$ as a function of frequency and adulterant percentage is derived (see ***Figure 2b***). ***Figure 2c*** shows predicted transmission coefficients from the function compared with measured transmission coefficients for a 0.03 percent concentration of detergent in distilled water. By comparing the measured transmission characteristics with the pre-trained reference curves, the adulterant concentration in the test sample is quantitatively estimated and predicted based on the measurement of $|S_{21}|$ (see ***Figure 2d***).

Because measurable decreases in $|S_{21}|$ versus frequency are observed with an increasing percentage of detergent in pure water, similar measurements are carried out with milk and different types of adulterants.

SAMPLE PREPARATION FOR MEASUREMENT

Measurements are made for two types of adulterants (i.e., solid and


MI-WAVE
Millimeter Wave Products Inc.
AEROSPACE | DEFENSE | COMMERCIAL
PASSIVE | ANTENNAS | SYSTEMS
Attenuators
Isolators & Circulators
Detectors
Filters
Waveguides
Calibration kits
Power Dividers/Combiners
Terminations
Adapters
Waveguide-to-Coax Adapters
Couplers
Conical Horns
Corrugated Conical Horns
Horn Lens Antennas
Omni Directional Antennas
Spot Focusing Antennas
Standard Gain Horns
Waveguide Probe Antennas
Wide Angle Scalar Horns
Assemblies
Subsystems
Custom Products
Prototypes
Mass Volume Production
MADE IN THE U.S.A. WITH PRIDE
CELEBRATING 36 Years IN BUSINESS
CERTIFIED ISO 9001-2015 COMPANY
2007 Gandy Blvd N Suite 1310
St. Petersburg, FL 33702
Tel: (727) 563-0034
Email: sales@miwv.com

liquid). For solid adulterants of detergent and starch, concentrations in the range of 1 to 10 percent (weight/volume) of pure double-toned milk are used. One gram of adulterant is added in ten consecutive steps to 100 ml of pure double-toned milk in a thin plastic box. Measurements are taken at each step, starting from pure milk (calibrated as the standard) and continuing until the adulterant concentration reaches 10 percent.

For a liquid adulterant, water (as the adulterant) is mixed with pure milk in volumetric ratios (i.e, volume/volume). Starting with a 5/100 concentration (i.e., 5 ml of distilled water in 100 ml of pure milk) and ending with a 100/100 concentration (i.e., 100 ml of distilled water in 100 ml of pure milk), twenty consecutive measurements are taken at equal intervals.

The above measurements are performed on relatively large concentrations of adulterants considered to be macro-level concentrations. Measurements are also performed using very small (micro-level) concentrations of detergent in pure double-toned milk, from 0.01 to 0.1 percent. The results show that the detection of micro-quantities of adulterants in liquid food items is also possible.

The measurement setup for macro- and micro-level measurements is the same. The cross-sectional dimensions of the flat box are unchanged at 25 by 16 cm^2. The only difference is the depth of the sample liquid. For macro-level measurements, the depth of the liquid is 0.25 cm, creating a total volume of 100 ml. For micro-level measurements, the depth of the liquid is 1 cm, creating a total volume of 400 ml. Impurities in milk can, therefore, be determined in macro as well as micro concentrations using the same technique. The measured results, in each case, show similar trends.

RESULTS AND ANALYSIS

Measurements of starch dissolved in milk are shown in ***Figure***

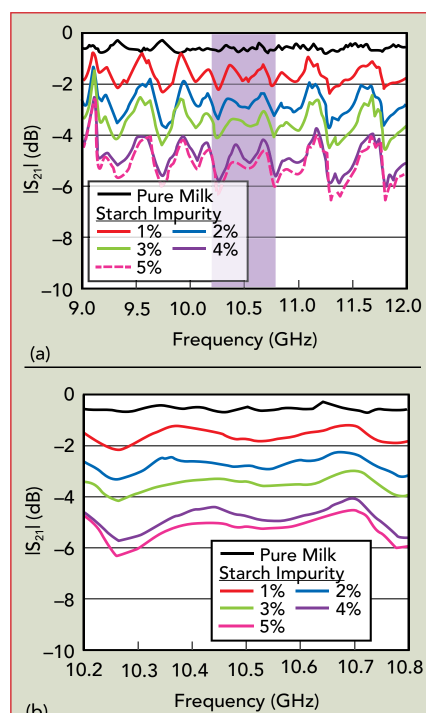

Fig. 3 **Measured $|S_{21}|$ from 9 to 12 GHz (a), and the same measurement shown from 10.2 to 10.8 GHz (b).**

3. Measured $|S_{21}|$ for increasing concentrations of starch as the adulterant in pure double-toned milk measured from 9 to 12 GHz is shown in ***Figure 3a***, where $|S_{21}|$ of pure double-toned milk is used as the reference. $|S_{21}|$ decreases monotonically with a 1 to 5 percentage point increase in the concentration of starch. The portion of the curve, from 10.2 to 10.8 GHz, is selected to more clearly illustrate the trend (see ***Figure 3b***).

The effect on $|S_{21}|$ of increasing concentrations of detergent is plotted in ***Figure 4***, while that of water as a liquid adulterant is shown in ***Figure 5***. In both cases, the trend is similar; $|S_{21}|$ decreases with an increasing percentage of adulterant.

$|S_{21}|$ for micro levels of detergent as an adulterant in pure double-toned milk is plotted in ***Figure 6***. The percentage of detergent adulterant varies from 0.03 to 0.08 percent in steps of 0.01 percent. This shows that very low levels of impurities in milk can be detected with this technique as well.

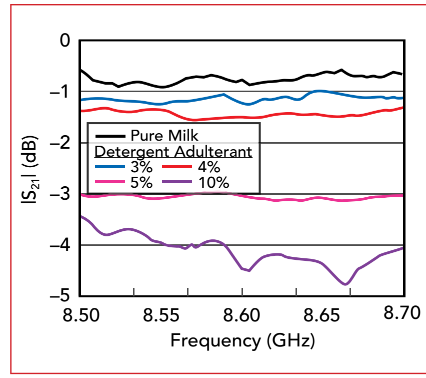

Fig. 4 **Measured $|S_{21}|$ for increasing concentrations of detergent.**

DISCUSSION

By measuring the transmission of microwave radiation through small quantities of adulterated milk, the concentration of its adulterants can be measured. When starch, detergent or water is added to milk, its dielectric constant increases monotonically with the increasing percentage of adulterant.[18,19] As the relative permittivity increases, in turn, $|S_{21}|$ decreases.[17]

The process can be extended to detect adulterants in other liquid food products like juices, beverages, drinks and edible oils. Even contaminants present in very small amounts in drinking water can be detected, as measurements in distilled water confirm. Various harmful chemicals, industrial waste and agricultural byproducts, such as heavy metals, fertilizer and pesticide residues, can contaminate water. These kinds of impurities are often present in small concentrations and pose serious health complications in drinking water or water used for other purposes.

The approach described here can be of enormous help in detection. It is relatively simple and less time-consuming than other methods. Concentrations of impurities can be measured based on a simple graphical technique without the need for expert food analysis.

CONCLUSION

This process has a crucial indus-

HIGH POWER COUPLERS

5 - 500 Watts

Model #	Frequency (MHz)	Coupling (dB) [Nom]	Coupling Flatness (dB)	Mainline Loss (dB) [Typ./Max.]	Directivity (dB) [Typ./Min.]	Input Power (Watts) [Avg.]
SDCHP-125	10 - 250	18.5	0.5	0.1 / 0.4	24 / 19	30
SDCHP-140	10 - 400	18.75	1	0.5 / 0.85	27 / 22	25
SBCHP-1100	10 - 1000	10	0.5	1.2 / 1.4	17 / 15	5
KBK-HP-1100	10 - 1000	10	0.5	1.2 / 1.4	17 / 15	5
KDK-HP-255	20 - 550	20	0.4	0.25 / 0.35	23 / 18	27.5
SDCHP-255	20 - 550	20	0.4	0.25 / 0.35	23 / 20	27.5
SDCHP-335	30 - 350	20.1	0.85	0.24 / 0.32	24 / 20	75
SDCHP-484	40 - 840	19.2	0.9	0.3 / 0.4	24 / 20	30
SCCHP-560	50 - 560	14.6	0.7	0.48 / 0.65	23 / 20	75
SCCHP-990	90 - 900	15.2	0.6	0.52 / 0.64	20 / 17	38.3
SBCHP-2080	200 - 800	12.3	0.7	0.64 / 0.80	24 / 18	48.3
SBCHP-2082	200 - 820	11.0	0.5	0.74 / 0.9	22 / 19	22.5
KDS-30-30-3	27 - 512	27.5	0.75	0.3 / 0.4	23 / 15	50
KDS-30-30	30 - 512	27.5	0.75	0.3 / 0.4	23 / 15	50
KBK-10-225	225 - 400	11	0.5	0.6 / 0.7	25 / 18	50
KBS-10-225	225 - 400	10.5	0.5	0.6 / 0.7	25 / 18	50
KDK-20-225	225 - 400	20	0.5	0.2 / 0.4	25 / 18	50
KDS-20-225	225 - 400	20	0.5	0.2 / 0.4	25 / 18	50
KEK-706H	500 - 2500	31.5	2.5	0.28 / 0.4	18 / 12	100
SCS-8012D	800 - 1200	20	0.6	0.22 / 0.25	22 / 18	100
KEK-704DH-2	850 - 1250	30	0.25	0.20 / 0.30	28 / 25	500
KEK-704H	850 - 960	30 5	0.25	0.08 / 0.20	38 / 30	500
SCS100800-10	1000 - 8000	10.5	2	1.2 / 1.8	8 / 5	25
SCS100800-16	1000 - 7800	16.8	2.8	0.7 / 1	14 / 5	25
SCS100800-20	1000 - 7800	20.5	2	0.4 / 0.75	12 / 5	25
SCS-1522B	1500 - 2200	10	--	0.65 / 0.75	23 / 18	100
SCS-1522D	1500 - 2200	20	--	0.32 / 0.38	23 / 20	100
SCS1701650-16	1500 - 15500	17	2.5	1 / 1.4	16 / 5	25
SCS1701650-20	1700 - 15000	21	2.5	0.9 / 1.3	10 / 7	25
SDC360440-10	3600 - 4400	8.6	0.25	0.7 / 1.4	18 / 10	10
SDC360440-20	3600 - 4400	19	0.25	0.7 / 1.2	16 / 10	10

New Models!

Talk To Us About Your Custom Requirements

SYNERGY®
MICROWAVE CORPORATION

Phone: (973) 881-8800 | Fax: (973) 881-8361
E-mail: sales@synergymwave.com | Web: www.synergymwave.com
Mail: 201 McLean Boulevard, Paterson, NJ 07504

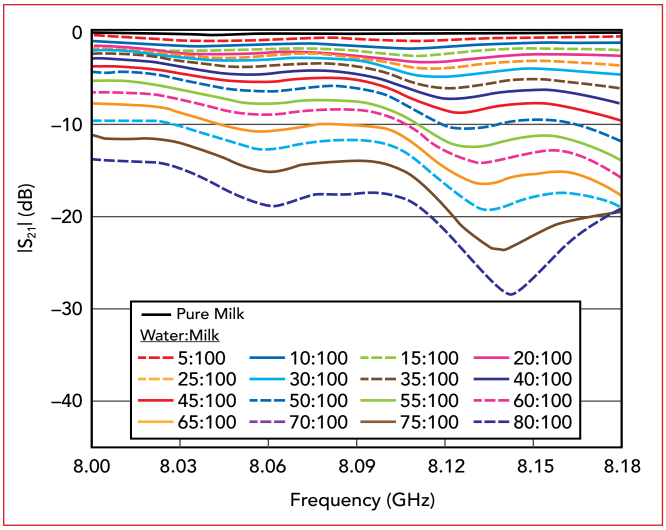

Fig. 5 **Measured $|S_{21}|$ for increasing concentrations of water.**

trial application. In the processing and packaging of food products in mass quantities, prior knowledge of the nature of their microwave transmission characteristics can be an indication of their purity/quality.

The quality of liquid food products can be checked with this method before commercial sale. This investigation has shown that it is possible to identify detergent, for example, in pure double-toned milk in proportions as low as 0.03 percent by weight of fresh milk. Modifications to the measurement setup can be made for greater accuracy and precision. It may also be possible to perform non-intrusive detection without opening the food package.

This process can be extended beyond food articles, for example, it may be useful for the detection of the percentage of components or impurities in crude oil or the detection of foreign elements in blood and other body fluids by medical diagnostic laboratories. ■

References

1. S. Bansal, A. Singh, M. Mangal, K. A. Mangal and S. Kumar, "Food Adulteration: Sources, Health Risks and Detection Methods," *Critical Reviews in Food Science and Nutrition*, Vol. 57, No. 6, April 2017, pp. 1174-1189.
2. S. Nirwal, R. Pant and N. Rai, "Analysis of Milk Quality, Adulteration and Mastitis in Milk Samples Collected from Different Regions of Dehradun," *International Journal of PharmTech Research*, Vol. 5, No. 2, June 2013, pp. 359-364.
3. A. Tanzina and A. Shoeb, "Common Milk Adulteration and Their Detection Techniques," *International Journal of Food Contamination*, Vol. 3, No. 22, December 2016.
4. B. S. Berry, C. S. Fernandes, A. Rajaratnam, S. N. DeChiara and R. C. Mace, "Measurement of the Hematocrit Using Paper-Based Microfluidic Devices," *Lab on a Chip*, Vol. 16, No. 19, September 2016, pp. 3689-3694.
5. C. J. Moore, J. Spink and M. Lipp, "Development and Application of a Database of Food Ingredient Fraud and Economically Motivated Adulteration from 1980 to 2010," *Journal of Food Science*, Vol. 77, No. 4, April 2012, pp. 118-126.
6. L. Mu, M. Dawande and V. Mookerjee, "Improving the Milk Supply Chain in Developing Countries: Analysis, Insights and Recommendations," *Production and Operations Management*, Vol. 23, No. 7, July 2014, pp. 1098-1112.
7. P. Singh and N. Gandhi, "Milk Preservatives and Adulterants: Processing, Regulatory and Safety Issues," *Food Reviews International*, Vol. 31, No. 3, February 2015, pp. 236-261.

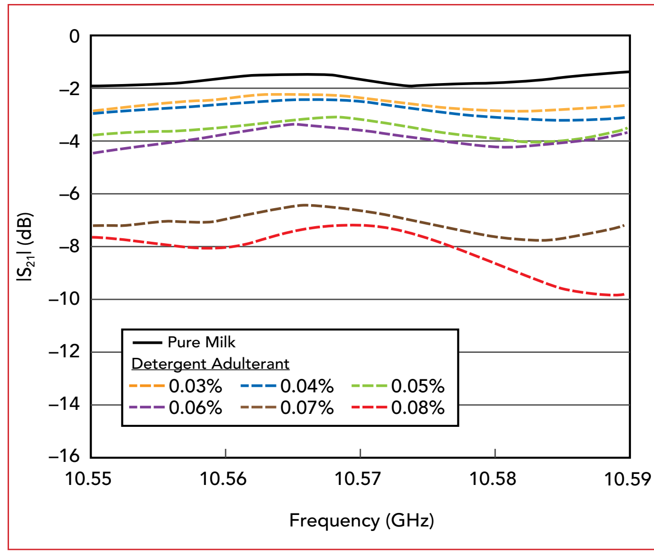

Fig. 6 **Measured $|S_{21}|$ for increasing micro-level concentrations of detergent.**

8. D. R. Maheswara, K. Venkatesh and S. V. C. Reddy, "Adulteration of Milk and its Detection: A Review," *International Journal of Chemical Studies*, Vol. 5, No. 4, 2017, pp. 613-617.
9. J. F. O'Hara, R. Singh, I. Brener, E. Smirnova, J. Han, A. J. Taylor and W. Zhang, "Thin-Film Sensing with Planar Terahertz Metamaterials: Sensitivity and Limitations," *Optical Express*, Vol. 16, No. 3, January 2008, pp. 1786-1795.
10. W. Withayachumnankul, H. Lin, K. Serita, C. M. Shah, S. Sriram, M. Bhaskaran, M. Tonouchi, C. Fumeaux and D. Abbott, "Sub-Diffraction Thin-Film Sensing with Planar Terahertz Metamaterials," *Optics Express*, Vol. 20, No. 3, January 2012, pp. 3345-3352.
11. M. H. Zarifi and M. Daneshmand, "Wide Dynamic Range Microwave Planar Coupled Ring Resonator for Sensing Applications," *Applied Physics Letters*, Vol. 108, No. 23, June 2016.
12. A. M. Albishi and O. M. Ramahi, "Highly Sensitive Microwaves Sensors for Fluid Concentration Measurements," *IEEE Microwave and Wireless Components Letters*, Vol. 28, No. 4, April 2018, pp. 287-289.
13. M. H. Zarifi and M. Daneshmand, "High-Resolution RFID Liquid Sensing Using a Chipless Tag," *IEEE Microwave and Wireless Components Letters*, Vol. 27, No. 3, March 2017, pp. 311-313.
14. L. Iram, M. Y. Sandhu, A. K. M. Z. Hossain and S. Khan, "Portable Real-Time Microwave Milk Quality Monitoring Sensor," *Proceedings of the 9th International Conference on Computer and Communication Engineering (ICCCE)*, August 2023, pp. 167-172.
15. A. Sadat, P. A. Mustajab and A. I. Khan, "Determining the Adulteration of Natural Milk with Synthetic Milk Using AC Conductance Measurement," Journal of Food Engineering, Vol. 77, No. 3, December 2006, pp. 472-477.
16. G. Durante, W. Becari, F. A. S. Lima and H. E. M. Peres, "Electrical Impedance Sensor for Real-Time Detection of Bovine Milk Adulteration," *IEEE Sensors Journal*, Vol. 16, No. 4, January 2015, pp. 861-865.
17. K. Zhang, J. Fu, L. Y. Xiao, Q. Wu and L. -W. Li, "Total Transmission and Total Reflection of Electromagnetic Waves by Anisotropic Epsilon-Near-Zero Metamaterials Embedded with Dielectric Defects," *Journal of Applied Physics*, Vol. 113, No. 8, February 2013.
18. D. Worku, M. Sharma, P. Kumar and B. Koteswararao, "Detection of Adulteration in Milk Using Capacitor Sensor with Especially Focusing on Electrical Properties of the Milk," *Proceedings of the 7th International Electronic Conference on Sensors and Applications*, November 2020.
19. Y. Smirnov, Y. Shestopalov and D. Mironov, "Analysis of Inverse Scattering in a Waveguide Using the Method of Volume Singular Integral Equation," *URSI International Symposium on Electromagnetic Theory*, August 2010.

MiCable

18~67GHz

32 Way ULTRA WIDEBAND POWER DIVIDER/COMBINER

NEW

5G, Test & Measurement, Instruments, Antenna Feed Network & Signal Distribution System etc.

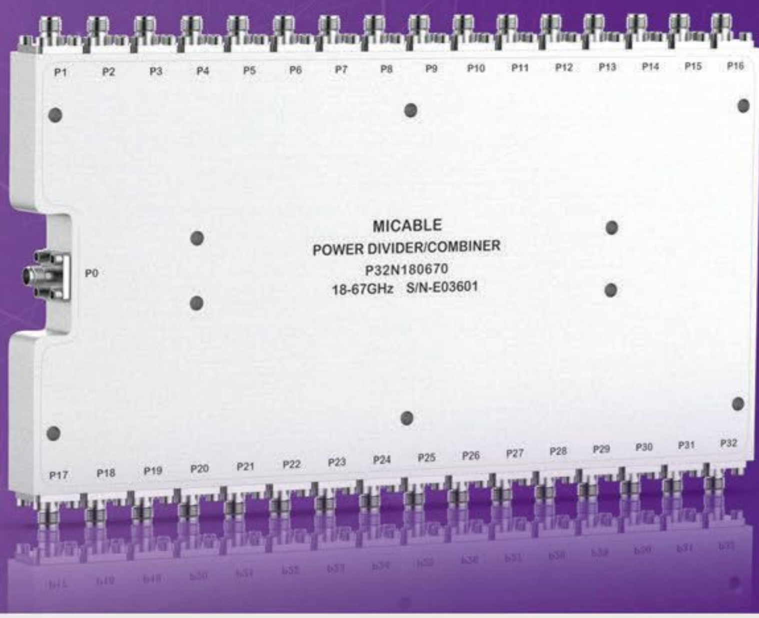

1-9 PCS

$10,099

- Frequency Range: 18~67GHz
- Low VSWR / Low I. L. / High Isolation
- Excellent Amplitude & Phase Unbalance

P/N	P32N180670
Way	32
Freq. Range	18~67GHz
Sum VSWR	1.8:1 (Max.)
Distri. VSWR	1.8:1 (Max.)
Insertion Loss*	9.4 dB(Max.)
Amplitude Unbal.	±0.8 dB(Max.)
Phase Unbal.	±12 Deg.(Max.)
Isolation	18 dB(Min.)
Dimension	110×210×14.0mm

* Above Theoretical Loss 15dB

Test Curve

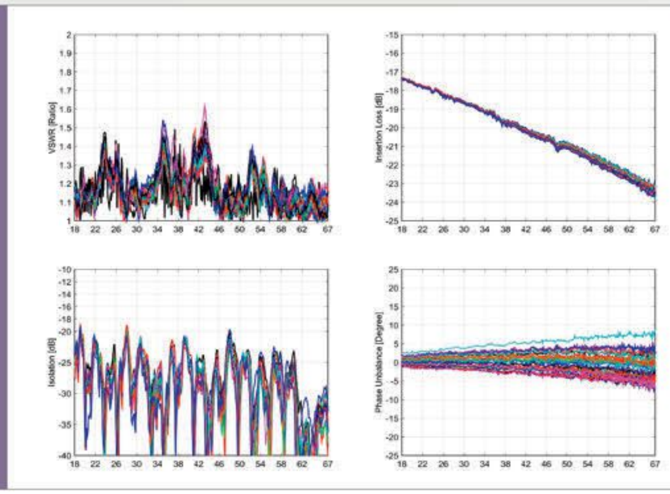

More Information- Scan the QR Code

MIcable Inc.

www.micable.cn sales@micable.cn +86-591-87382856

Multichannel GHz Digitizers

Spectrum Instrumentation GmbH
Grosshansdorf, Germany

Spectrum Instrumentation has introduced new digitizers with a maximum of 12 channels, offering up to 5 Gigasamples per second (GSPS) sampling speed, or up to six channels at 10 GSPS. The new DN6.33x digitizers are part of Spectrum Instrumentation's Netbox series, a user-friendly instrument line that requires only an Ethernet cable to be controlled from any PC, laptop or network. A comprehensive software package and several hardware features make them compatible with automated testing applications, capturing signals on multiple synchronized inputs. With 15 new variants, Spectrum now offers a total of 94 different digitizer Netboxes, ranging from 5 MSPS to 10 GSPS acquisition speed.

Each channel of a DN6.33x digitizer is equipped with a 12-bit analog-to-digital converter (ADC) that samples at up to 3.2, 6.4 or 10 GSPS, with an analog bandwidth of 1, 2 and 3 GHz, respectively. Customers can choose from a selection of models offering 4, 6, 8, 10 or 12 synchronous channels, with up to six channels available in the 10 GSPS configurations. This flexibility lets users tailor the system to fit specific test setups, without needing to pay for excess channels or bandwidth. If only one or two of these fast channels are required, Spectrum offers the smaller DN2.33x Netbox series.

Spectrum designed the DN6.33x series to meet the needs of research and industrial users seeking a reliable and easy-to-integrate solution. These instruments include everything required to capture, store and analyze high speed electronic signals. Users can connect the digitizer directly to a PC, laptop or company network using a standard Ethernet or LXI connection.

Each input channel on the DN6.33x series features its own ADC and independently programmable front-end electronics. This design maximizes dynamic range and measurement accuracy. Users can set input ranges in four steps from ±200 mV up to ±2.5 V with additional support for signal offset and calibration. Since all ADCs operate synchronously, users benefit from timing alignment across all channels, which is critical for phase-sensitive applications such as array measurements and modulation analysis. The internal system clock provides precision, with an accuracy better than ±1 part per million (ppm). The digitizers are equipped with Gigasamples of on-board memory, allowing long or complex signal captures to be stored at high resolution. For all models, every two channels are provided with 2 Gigasamples of memory as standard, with an optional upgrade to 8 Gigasamples. At the maximum speed of 10 GSPS and full memory size, users can capture signals up to 800 microsecond in duration in a single acquisition. Each data point in the waveform is spaced just 100 picoseconds apart.

To support efficient data capture and analysis, the DN6.33x series

Fig. 1 Analysis of a modulated 1 GHz carrier quadrature.

offers a suite of advanced acquisition and triggering modes. Features such as transient recording, multiple recording and optional block averaging help users capture key signal events and store them with precision timing. These tools are useful when analyzing rare or unpredictable signal behaviors, where memory efficiency and timing accuracy directly impact test success.

Software support is another key attribute of the DN6.33x platform. Every unit includes SBench 6 Professional, Spectrum's software tool for acquisition, display, processing, analysis and documentation. For developers building custom applications, full programming support is provided through a software development kit that is compatible with a wide range of programming environments, including C++, Python, MATLAB and LabVIEW.

The system's accessible front-panel connectors allow for integration into automated test equipment. The connectors allow for straightforward connection of external clock and trigger sources and support various digital I/O functionalities. Users can implement asynchronous and synchronous digital inputs, output status flags and other control signals. An optional high speed digital pulse generator is also available. For users planning permanent setups, mounting kits are available for standard 19 in. racks, helping ensure a clean and stable installation.

Thanks to their performance and flexible configuration, DN6.33x digitizers are suited for a wide range of applications in communications, aerospace, defense, scientific research, photo-voltaic analysis and semiconductor testing. For users working on MIMO communications, phased-array radar or time-correlated measurements, the system's channel synchronization is a significant advantage.

In a practical example, one of the digitizers in the series, the DN6.335, was used to analyze an 8PSK-modulated 1 GHz carrier signal, as shown in ***Figure 1***. In Figure 1, the upper left trace is the acquired 8PSK signal, with horizontal zooms of that trace displayed to the right. The lower left trace shows the spectrum of the signal with expanded views to the right. With the digitizer sampling at 10 GSPS, a 20 microsecond portion of the waveform was captured. Using the SBench 6 software, users could examine the waveform, observe the frequency spectrum including the modulation envelope and see the third harmonic of the carrier at 3 GHz, attenuated by approximately 36 dB relative to the primary peak. With built-in cursor and zoom tools, SBench 6 allows detailed inspection of timing, spectral features, sidebands and filter effects without needing to export the data.

In addition to their technical strengths, the DN6.33x series digitizers are built for longevity and user confidence. Every unit carries a five year warranty, with free lifetime access to software and firmware updates. Spectrum Instrumentation also provides direct support from all hardware and software engineers. For users investing in long-term test platforms, the 15 to 20 years of committed service and parts availability offer peace of mind.

VENDORVIEW

Spectrum Instrumentation GmbH
Grosshansdorf, Germany
www.spectrum-instrumentation.com

New Rad-Hard GaN HEMT for Next Generation Missions in Space

Infineon Technologies IR HiRel
Andover, Mass.

The demand for greater communication bandwidth on a global scale is growing. As a result, next-generation satellites must deliver higher data throughput for digital payloads. Among in-orbit configurations, edge computing and other advanced needs, current FPGAs and ASICs call for greater power requirements. The shift to digital payloads requires engineers to reassess key design parameters, such as material needs, operational factors and radiation robustness, to ensure reliable performance in their space power systems.

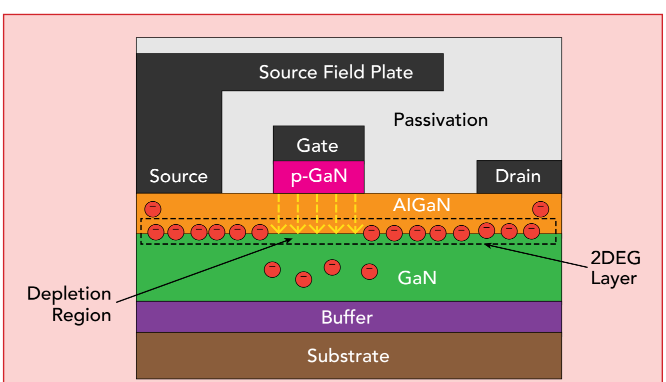

Fig. 1 **Cross-sectional structure of GaN HEMT.**

For generations, silicon (Si) has been the industry's material of choice in power applications; however, in recent years, GaN has shown promise, offering a multitude of advantages in applications where reaching high switching speeds and efficiency are equally as important as minimizing the size and weight of a power system. GaN use in space applications is expanding due to the benefits of using a wider bandgap semiconductor to optimize operations and its performance as a radiation-hardened (rad-hard) high electron mobility transistor (HEMT). Infineon IR HiRel manufactures rad-hard GaN transistors with JANS qualification.

TECHNOLOGICAL ARCHITECTURE OF GAN

GaN holds a bandgap energy of 3.4 eV. In comparison, legacy technology, such as Si, has a bandgap

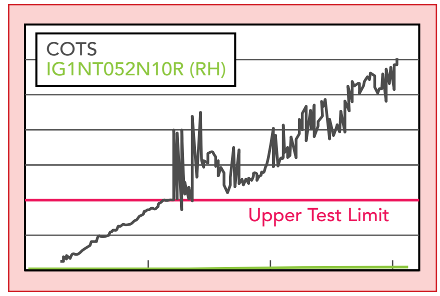

Fig. 2 SEE flux radiation versus drain-source leakage current.

energy of 1.1 eV. The material properties of wide bandgap semiconductors such as GaN make the technology suitable for power transistors. ***Figure 1*** illustrates the general design of Infineon IR HiRel's lateral GaN HEMT, IG1NT052N10R. Electrons move from the source to the drain through a 2-dimensional electron gas (2DEG) layer formed at the AlGaN and GaN epi heterojunction layer. This is a result of a piezoelectric effect that occurs at the interface between the two layers. A layer of positively doped GaN, p-GaN, is integrated between the gate and AlGaN layer to produce a depletion region. The inclusion of a p-GaN layer allows the transistor to have a positive threshold voltage and perform as an enhancement-mode device. This structure plays a role in the benefits of GaN as a power transistor technology. The source field plate reduces the peak electric fields found on the gate. The 2DEG layer allows high mobility of electrons with minimal drain-source resistance ($R_{DS(on)}$), a key parameter to account for in power transistors. Low V_{th}, such as 1.5 V for IG1NT052N10R, results in higher switching speeds. The structure of a lateral GaN HEMT also lacks a gate oxide that is typically observed in Si MOSFETs. As a result, GaN has a slight robustness to radiation inherent to its design. However, rad-hard by design is still applicable to GaN, as some parameters need to be mitigated under radiation.

RADIATION AND POWER PERFORMANCE

There is some inherent robustness to GaN under various radiation effects due to the absence of a gate oxide. GaN faces no trapped charge nor $V_{GS(th)}$ shift under total ionizing dose (TID) radiation and does not suffer from single event gate rupture (SEGR) under single event effect (SEE). Even though GaN has inherent radiation resistance, there is still an advantage to choosing rad-hard solutions over commercial-off-the-shelf (COTS) parts for space applications. ***Figure 2*** demonstrates the

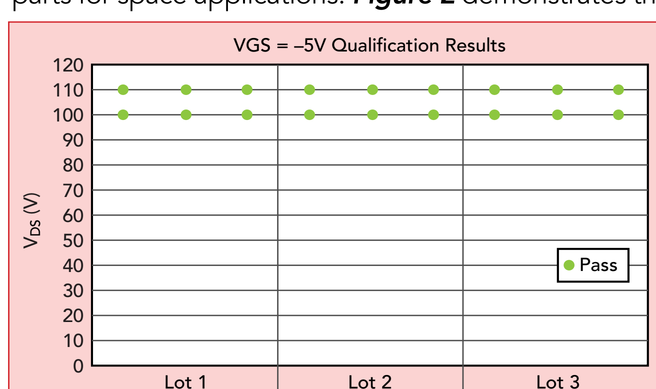

Fig. 3 SEE SOA for IFX IR HiRel 100 V RH GaN HEMT.

Fig. 4 3D representation of PowIR-SMD.

importance of creating a GaN transistor that is rad-hard by design. Comparing a COTS-graded GaN to a rad-hard GaN, it is observable that the COTS device significantly drifts while the rad-hard GaN remains relatively stable over the entire duration. Radiation hardened by design will often ensure the reliability required in extreme environment applications. ***Figure 3*** highlights the radiation robustness of GaN under SEE for three different lots tested up to Au. In addition to how the GaN device under testing does not require derating when subjected to LET of 70 MeV*cm^2/mg (the LET Si equivalent to 86.5 MeV*cm^2/mg), the electrical operation of the device is up to standard with the industry's leading rad-hard transistor standards. To make sure the device is suitable for power architectures in space systems, Infineon IR HiRel created a new package specifically for GaN, called the PowIR-SMD.

PACKAGING

Infineon IR HiRel developed a new surface-mount package to ensure reliability and robust operations for its rad-hard GaN device. Minimizing parasitic inductance is imperative in system design because GaN is a fast-switching technology. Infineon IR HiRel developed the PowIR-SMD to be a bond wire-free SMD package that has an inductance value of 0.1 nH. Additionally, this package allows a Kelvin-source connection to decouple the gate drive from the power stage, lowering the common-source inductance of the device.

Another factor to address is the CTE mismatch between the packaged device and the PCB. Occasionally, ceramics such as alumina are developed into hermetic packaging to address such mismatches. This is seen with Si MOSFETs, where the devices are large enough to dissipate the heat generated. The high density of GaN allows the technology to perform efficiently within a smaller form factor compared to Si MOSFETs. Consequently, packages dedicated to GaN would benefit from developing a package consisting of aluminum nitride, AlN. The higher thermal conductivity of AlN compared to alumina, 150 W/m*K versus 12 W/m*K, respectively, allows the device to dissipate heat more effectively. The size of GaN, in this case, is small enough to mitigate the thermal cycling mechanical stress concern that is considered when using AlN. The inclusion of AlN holds an additional benefit as it lessens the accumulation of free charges from environmental radiation, preventing system damage and contributing to inherent radiation robustness. ***Figure 4*** illustrates a 3D representation of a hermetic package, PowIR-SMD, a surface-mount packaging dedicated to addressing GaN usage in space.

CONCLUSION

The increasing demand for higher processing power in satellites has led to a growing need for advanced technologies that can handle complex tasks such as artificial intelligence, in-orbit reconfiguration and more. High-power FPGAs and ASICs are being driven to their limits, and as a result, improved efficiency and reduction in size and weight are critical factors to consider in satellite design.

Infineon IR HiRel's rad-hard GaN HEMT brings radiation performance and electrical robustness to the high-reliability market. The 100 V rad-hard GaN HEMT, now available under MIL-PRF-19500 JANS qualification, has been designed to optimize performance in power systems.

Infineon Technologies
IR HiRel
Andover, Mass.

8-Way SMT Bandpass Filter Bank

The FB010BW16SG from ED2 is an eight-way bandpass filter bank designed to cover the 2 to 18 GHz frequency range in discrete 2 GHz increments. Internally matched to 50 Ω and housed in a 9 mm × 9 mm SMT LGA package, this filter bank offers -4 dB typical insertion loss, 30 dB of rejection or greater for each filter and a 20 ns switching speed, making it ideal for low SWaP designs in defense and aerospace systems.

Each channel provides a typical insertion loss of 4 dB with return loss exceeding 12 dB while maintaining a maximum continuous wave input power of +30 dBm. Drawing 15 mA from a ±5 V supply and switching between bands in 20 ns, the FB010BW16SG enables high speed agility in applications like EW receivers, SIGINT platforms, radar warning systems and wideband communications modules. Its form factor and rugged temperature range from –40°C to +85°C make it suitable for integration into size-constrained platforms such as UAV payloads and embedded mission systems.

ED2 uses advanced substrate technology and has a vertically integrated design approach. ED2 architectures are engineered from the ground up to balance RF performance, thermal management and manufacturing scalability. Their in-house expertise spans embedded processing, custom packaging and ultra-wideband RF design, enabling products that meet stringent defense and commercial wireless requirements.

With frequency coverage from 20 MHz to 94 GHz and proven capability across tactical and next-gen systems, ED2 offers RF designers a robust, scalable path to deployment. The FB010BW16SG exemplifies this philosophy, performing in a footprint built for mission-critical environments.

Available now from RFMW.

VENDORVIEW

RFMW, San Jose, Calif.
https://www.rfmw.com/manufacturer/ed2

ED2, Tucson, Ariz.
www.ed2corp.com

RadioVerse® Transceivers: Balanced Power and Performance

ADI's new RadioVerse Transceivers contain advanced architectures for balancing power and BW performance coupled with high channel count and optimal digital capability.

Analog Devices Inc.

https://www.analog.com/en/resources/media-center/videos/6375180705112.html

ETS-Lindgren Named to Newsweek's America's Greatest Midsized Workplaces 2025

ETS-Lindgren announced that it has been recognized as one of America's Greatest Midsized Workplaces 2025 by *Newsweek* and Plant-A Insights Group. *Newsweek* and Plant-A Insights Group recognize companies through a rigorous evaluation based on online employee reviews, publicly available data, an extensive survey and over 120 key performance indicators.

ETS-Lindgren

www.ets-lindgren.com

RF/Microwave Micro-Ceramic Filters for Stripline, Microstrip and Co-Planar Waveguide (CPWG) Launches

RF Design Engineer William Yu explains the different implementations of Mini-Circuits micro-ceramic (LTCC) filters in this demo from Mini-Circuits' engineering lab in Brooklyn, N.Y.

Mini-Circuits

https://blog.minicircuits.com/rf-microwave-micro-ceramic-filters-for-stripline-microstrip-and-co-planar-waveguide-cpwg-launches/

Taking Advantage of Discrete Optimization

Discrete optimization is an available feature when using Keysight ADS combined with Modelithics Microwave Global Models™ for RLC components. In this blog post, learn how you can take advantage of this feature to allow part values to be automatically adjusted to optimal real-life manufacturer part values.

Modelithics

www.modelithics.com/FreeDownloads/Blogs/Modelithics_Model_Rap_August2025_Final.pdf

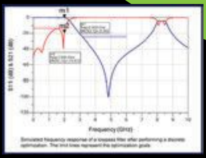

Precision in Under 5 Minutes – Tips and Tricks on EMI Debugging

In this video, Masha shares practical EMI debugging tips and demonstrates how to effectively use these tools for comprehensive EMI troubleshooting, ensuring your projects run smoothly and efficiently.

Rohde & Schwarz

www.youtube.com/watch?v=aTvIcaa3KUc

New Space Brochure

Smiths Interconnect released their new brochure of connectivity products for the space industry where the company spotlights all their heritage in space exploration developing market-leading technology solutions.

Smiths Interconnect

www.smithsinterconnect.com/markets/space/

NEW PRODUCTS

FOR MORE NEW PRODUCTS, VISIT WWW.MWJOURNAL.COM/BUYERSGUIDE
FEATURING VENDORVIEW STOREFRONTS

DEVICES/ COMPONENTS/MODULES

Illuminated Miniature Rocker Switches

The RN series rocker switches from CIT Relay and Switch are miniature in size and yet rugged and reliable. With multiple switch function options, the RN series offers a black, white or gray housing, with a multitude of actuator choices, including transparent options. With 10 marking options, these 20 A rocker switches are ideal for use in telecommunications, computer peripherals, audio/visual, instrumentation, and nearly any low-power design.

Digi-Key
www.digikey.com

6501 Series Up/Down Converters

The 6501 Series Converters deliver two fully independent RF Up/Down channels in a single 3U VPX slot, reducing SWaP (size, weight, and power) without compromising performance. Designed for mission-critical environments, it supports fast switching, wide frequency coverage, low phase noise, and high dynamic range—making it ideal for EW, SIGINT, SATCOM, and radar applications. Get the 6501 Series Converters performance specs and discover how it can enhance your next mission-critical system.

FEI-Elcom Tech
www.fei-elcomtech.com

Isolators & Circulators

VENDORVIEW

JQL Technologies Corporation has launched space qualified surface-mount and microstrip isolators and circulators. These devices have gone through Group B qualification testing and screening per MIL-STD. Surface mount isolators are available from L-Band to Ku-Band and Microstrip isolators are available from C-Band to Ka-Band. JQL has built hundreds of these devices for LEO programs.

JQL Technologies Corporation
www.jqlelectronics.com

Surface Mount Bandpass Filter

VENDORVIEW

The MFBP-00086CSP3 passive MMIC surface mount bandpass filter is an ideal solution for small form factor, high rejection filtering. The MFBP-00086CSP3 features a 12.7-17.9 GHz 1 dBc passband and 1.9 dB center frequency insertion loss. Passive GaAs MMIC technology allows production of smaller filter constructions that replace larger form factor circuit board constructions. Tight fabrication tolerances allow for less unit-to-unit variation than traditional filter technologies. The MFBP-00086CSP3 is available in a 3.5 x 3.5 mm CSP3 chip scale package.

Marki Microwave
www.markimicrowave.com

Switch

VENDORVIEW

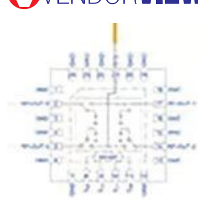

Mini-Circuits introduced the M4SWA4-34DR+ GaAs MMIC SP4T switch, supporting a wide variety of signal routing applications from DC to 30 GHz in a 4x4 mm QFN-style package. This model joins the M3SWA2-34DR+ SPDT model to give you even more high-performance options for signal routing in your system.

Mini-Circuits
www.minicircuits.com

Broadband Conical Inductors

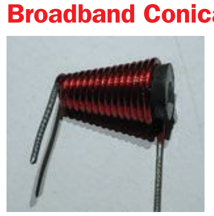

Passive Plus (PPI) has announced a new line of broadband conical inductors for bias Ts, broadband chip manufacturing, communication platforms, high frequency, microwave circuitry, RF test set-ups, test & measurement, test gear, test instrumentation and transmission amplifiers. These special RF chokes are used to filter RF and microwave frequency interference from electronic circuits in order to reduce EMI by attenuating high-frequency noise with an upper frequency limit up to 110 GHz (depending on substrate). S-Parameters are available on PPI's website.

Passive Plus
www.passiveplus.com

Programmable Resistor Modules

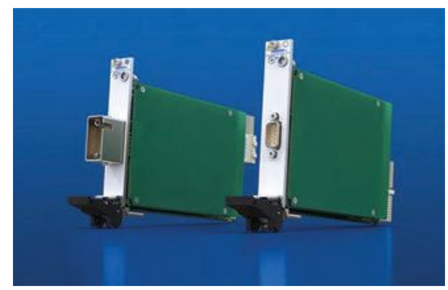

Pickering Interfaces announced a new family of high-voltage programmable resistor modules in a compact single-slot PXI and PXIe form factor, model 40-230 (PXI) and 42-230 (PXIe), providing a simple solution for applications requiring voltage handling up to 1.2 kV. Part of Pickering's expanding range of programmable resistor modules, the new module is available in 70 standard builds, including four single-channel builds that offer a wide variety of resistance ranges and resolution capabilities.

Pickering Interfaces
www.pickeringtest.com

10-bit Programmable 16 dB Attenuator

VENDORVIEW

Quantic PMI Model Number DTA-100M40G-15DB-10BIT is a 10-bit programmable 16 dB attenuator with step resolution of 0.015625 dB over the frequency range of 0.1 to 40 GHz with an attenuation accuracy of ±2.5 dB; insertion loss of 3 dB up to 20 GHz and 6 dB at 40 GHz; input 1 dB compression of 20 dBm and a VSWR of 2.5:1. Housing size is 2.0 x 1.8 x 0.5 in. with 2.92 mm (F) connectors.

Quantic PMI
www.quanticpmi.com

NewProducts

Switches

VENDORVIEW

Würth Elektronik expands its switch program. The popular SMT-mountable short-travel push-button switches are now joined by a new size version: the "WS-TASV SMT Tact Switch 4.5*3.2 mm". The switches are available in three versions with different actuation forces. The range of power switches is expanded with a rocker switch for a particularly space-saving device panel cut-out. The short-travel push-buttons from Würth Elektronik are suitable both for switching functions on and off as well as for use as signal transmitters.

Würth Elektronik
www.we-online.com

CABLES & CONNECTORS

Compact Surface-Mount SMB Jack

Amphenol RF introduced a new high performance surface-mount straight SMB jack into their broad portfolio of SMB connectors. With a true surface-mount footprint, this connector is designed with four gold-plated ground tabs that solder directly to the board for superior coplanarity and automated pick-and-place handling. This 50 Ohm jack features a drop-in footprint which makes it well-suited for industrial control modules, test and measurement equipment, avionics and military electronics equipment.

Amphenol RF
www.amphenolrf.com

DC~18 GHz High Performance Push-pull Quick-fit SMA Microwave Cable Assembly

VENDORVIEW

MIcable's high performance quick-fit SMA microwave cable assembly adopts spring claw design to get a feature of quick mounting to and quick separating from a regular SMA female connector. It's quite suitable for high volume product testing and increases test efficiency.

MIcable
www.micable.cn

AMPLIFIERS

6.0–18.0 GHz, 400 W, 200 W P1dB, a Rugged TWT Replacement

VENDORVIEW

Exodus AMP20178 is designed for EMI/RFI, lab, CW/Pulse, and all communication applications. A compact, rack-mounted Class A/AB linear amplifier utilizing high-power advanced technology devices. Covers 6.0–18.0 GHz with instantaneous ultra-wide bandwidth, 400W Typical output 200 W P1dB min. power, and 55dB gain. Built-in protection circuits with extensive monitoring of forward/reflected power, VSWR, voltage, current, and temperature. Local LCD and remote interface options available. In a reliable, efficient 7U chassis.

Exodus Advanced Communications
www.exoduscomm.com

Distribution Amplifiers

VENDORVIEW

HASCO Components announced their new line of high-performance distribution amplifiers manufactured by Esterline Research. These amplifiers include limiter circuits that not only provide fixed output levels but also offer high input gains. The input limiter is followed by three amplifier/low-pass filter stages, which ensure low-distortion sine wave outputs.

HASCO
www.hasco-inc.com

Broadband Amplifiers

VENDORVIEW

Rohde & Schwarz has expanded its broadband amplifier portfolio of the R&S®BBA300 family with the two innovative amplifier series R&S®BBA300-F for 6 to 13 GHz and R&S®BBA300-FG for 6 to 18 GHz with additional power classes such as 90 W, 180 W and 300 W. Together with the already successfully introduced broadband amplifier series R&S®BBA300-CDE and R&S®BBA300-DE, Rohde & Schwarz now offers compact dual-band amplifiers covering the entire frequency range from 380 MHz to 18 GHz in 4HU desktop models only.

Rohde & Schwarz
www.rohde-schwarz.com

New**Products**

SOURCES

Ka-Band Oscillator Tunes Across 8 GHz

VENDOR**VIEW**

Gunn-diode oscillator model SOF-2820-M1 tunes mechanically from 29.5 to 37.5 GHz. Typical output power is +18 dBm. Featuring a WR-28 waveguide output port and a female SMA bias-voltage input port, the oscillator requires +5 VDC at 850 mA. A micrometer tuner enables repeatable and stable frequency adjustment.

Eravant
www.eravant.com

Rugged 32.768 kHz TCXO for Fast GNSS Lock

VENDOR**VIEW**

The SiTime SiT7910 Endura™ Super-TCXO is the industry's most accurate 32.768 kHz TCXO, purpose-built for GNSS, defense, and rugged industrial systems. With ±0.1 ppm stability, ultra-low 5 µA power draw, and MEMS-based durability, it outperforms quartz in high-vibration, extreme-temperature environments. Its fast signal lock, 20 ppb/g g-sensitivity, and 2.1 ns jitter make it ideal for mission-critical timing in handheld radios, GNSS receivers, and high-reliability field equipment. Now available at RFMW.

RFMW
www.rfmw.com

TEST & MEASUREMENT

PE0312-75 Port Extender for 75 Ohm VNAs

VENDOR**VIEW**

The PE0312-75 Port Extender (or 12-Port 75 Ohm switch) is able to connect to CMT's SC7540 75 Ohm VNA to make multiport measurements in 75 Ohm systems. For users needing to measure 75 Ohm splitters with or without gain, insertion loss and isolation of a coaxial switch, or six simultaneous 2-port measurements in a production environment, a PE0312-75 is the perfect solution. The 12-Port PE0312-75 Port Extender has a frequency range from 3 MHz to 3 GHz and has a switching time of 1 ms typ.

Copper Mountain Technologies
www.coppermountaintech.com

High Bandwidth Oscilloscope Probes

VENDOR**VIEW**

Keysight Technologies, Inc. introduced the InfiniiMax 4 Series high bandwidth oscilloscope probes, expanding its portfolio of high frequency probes to cover bandwidths up to 52 GHz. As the industry's only solution with a high impedance probe head operating at more than 50 GHz, the InfiniiMax 4 Series provides digital designers with a turn-key probing solution for high speed digital, semiconductor and wafer applications.

Keysight Technologies, Inc.
www.keysight.com

Review by Dr. Ajay K. Poddar

Bookend

Chipless RFID Printing Technologies

Santanu Kumar Behera, Durga Prasad Mishra

The book "Chipless RFID Printing Technologies" explores the advancing field of wireless communications and printed electronics. It analyzes chipless RFID systems, emphasizing innovative printing techniques that could transform the industry. This publication serves as a timely resource in the evolving field of RFID systems, delivering a detailed overview that effectively bridges theoretical principles with practical applications. The text begins by outlining the advanced fundamentals of chipless RFID communication, exploring the crucial roles of sensors, reader antennas and radar cross-sections. It compellingly asserts the essential significance of RFID printing technologies in the creation of modern digital devices, thereby laying a strong foundation for a thorough technical discourse.

The book includes a detailed table of contents and is structured into nine chapters that cover key topics like Introduction, Literature Review and Smart Materials for Chipless RFID Printing. Each chapter focuses on printing methods and advanced materials to improve performance, cost efficiency and scalability, featuring diagrams, case studies and experimental results that illustrate the applications and limitations of chipless RFID technology, along with substrate selection for mass production.

The authors explore the production processes for RFID tags, including wireless sensors and conductive tags, highlighting the versatility of chipless RFID technology in biomedical and wearable applications. A key strength of this publication is its clear explanation of complex technical concepts and focus on sensing materials crucial for RFID printing, particularly passive printable resonators. They also examine innovative signal processing techniques that improve detection reliability. This blend of materials science and signal processing helps readers understand the creation of efficient, low-cost RFID solutions. By discussing emerging sensing strategies and advanced printing techniques, the book encourages further research in the field. "Chipless RFID Printing Technologies" serves as a vital resource for engineers and academics, providing a comprehensive overview and practical guidance for implementing advanced RFID solutions.

ISBN: 9781630819996
Pages: 310
Copyright: 2024
To order this book, contact:
Artech House
us.artechhouse.com

Advertising**Index**

Sales Representatives

Eastern and Central Time Zones
Carl Sheffres
Group Director
(New England, New York, Eastern Canada)
Tel: (781) 619-1949
csheffres@mwjournal.com

Michael Hallman
Associate Publisher
(NJ, Mid-Atlantic, Southeast, Midwest, TX)
Tel: (301) 371-8830
Cell: (781) 363-0338
mhallman@mwjournal.com

Pacific and Mountain Time Zones
Brian Landy
Western Reg. Sales Mgr.
(CA, AZ, OR, WA, ID, NV, UT, NM, CO, WY, MT, ND, SD, NE & Western Canada)
Tel: (831) 426-4143
Cell: (831) 713-9085
blandy@mwjournal.com

International Sales
Michael O'Kane
Tel: +44 (0) 1875 825 700
Cell: +44 (0) 7961 038 245
mokane@horizonhouse.com

Germany, Austria, and Switzerland (German-speaking)
Victoria and Norbert Hufmann
victoria@hufmann.info
norbert@hufmann.info

France
Gaston Traboulsi
Tel: +44 207 596 8742
gtraboulsi@horizonhouse.com

Korea
Jaeho Chinn
JES MEDIA, INC.
Tel: +82 2 481-3411
corres1@jesmedia.com

China
Shanghai
Linda Li
ACT International
Tel: +86 136 7154 0807
lindal@actintl.com.hk

Wuhan
Phoebe Yin
ACT International
Tel: +86 134 7707 0600
phoebey@actintl.com.hk

Shenzhen
Samuel Zhoul
ACT International
Tel: +86 186 8201 0368
samuelz@actintl.com.hk

Beijing
Cecily Bian
ACT International
Tel: +86 135 5262 1310
cecilyb@actintl.com.hk

Hong Kong
Floyd Chun
ACT International
Tel: +86 137 2429 8335
floydc@actintl.com.hk

Taiwan, Singapore
Simon Lee
ACT International
Tel: +852 2838 6298
simonlee@actintl.com.hk

Japan
Katsuhiro Ishii
Ace Media Service Inc.
Tel: +81 3 5691 3335
amskatsu@dream.com

Submitting ad material?
Visit: www.adshuttle.com/mwj
(866) 774-5784
outside the U.S. call
+1-414-566-6940

Ed Kiessling
(781) 619-1963
ekiessling@mwjournal.com

Corporate Headquarters: 685 Canton Street, Norwood, MA 02062 • Tel: (781) 769-9750

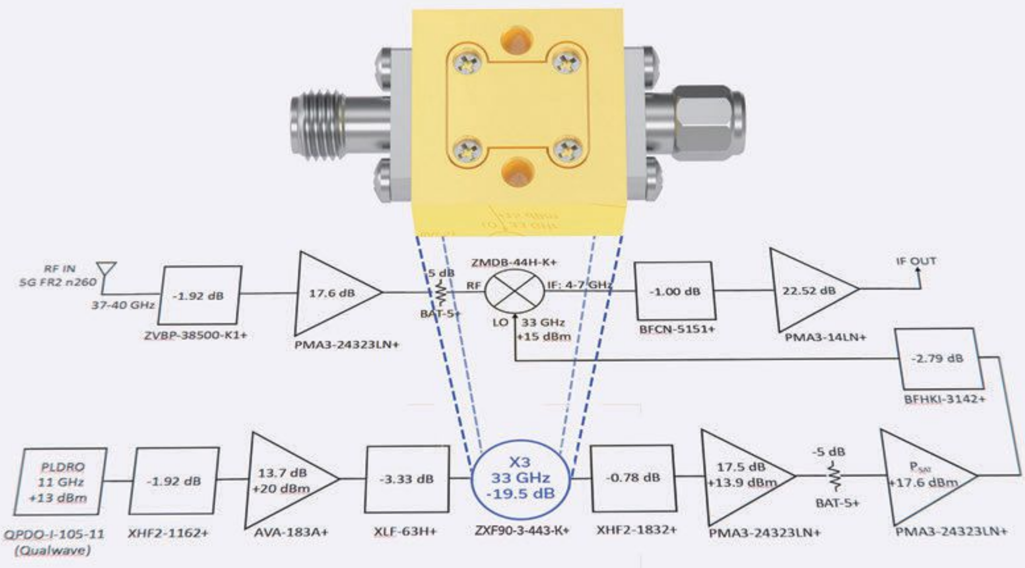

9 TO 72 GHz

Coaxial Frequency Multipliers

For High-Frequency LO Chains,
Upconverters & More

xN

High-frequency multipliers cover 9 to 72 GHz with +12 to +20 dBm input in compact, coaxial housings.

Model Name	Description	F Low	F High
ZXF90-3-223-K+	X3 Frequency Multiplier, SMA-F to 2.92 mm-M, 50Ω	10 GHz	22 GHz
ZXF90-3-443-K+	X3 Frequency Multiplier, SMA-F to 2.92 mm-M, 50Ω	20 GHz	43.5 GHz
ZXF90-3-453-V+	X3 Frequency Multiplier, SMA-F to 1.85 mm-M, 50Ω	20 GHz	45 GHz
ZXF90-3-64-E+	X3 Frequency Multiplier, 2.92 mm-F to 1.85 mm-M, 50Ω	30 GHz	60 GHz
ZXF90-3-723-E+	X3 Frequency Multiplier, 2.92 mm-F to 1.85 mm-M, 50Ω	40 GHz	72 GHz
ZXF90-2-44-K+	X2 Frequency Multiplier, 2.92 mm-F to 2.92 mm-F, 50Ω	12.4 GHz	40 GHz
ZXF90-2-153-K+	X2 Frequency Multiplier, 2.92 mm-F to 2.92 mm-F, 50Ω	9 GHz	15 GHz

LEARN MORE

Mini-Circuits®

FABS and LABS

KRYTAR: Celebrating 50 Years in the RF/Microwave Community

Thomas J. Russell, a broadband design expert who designed one of the first proprietary computer-aided engineering (CAE) tools, founded KRYTAR in 1975. KRYTAR designs and manufactures ultra-broadband mmWave, microwave and RF components and test equipment for both commercial and military wireless communications, radar, space and thermal vacuum applications. Russell has contributed to KRYTAR's success through a plethora of patented designs, including KRYTAR's first product, the Model 1816, a directional coupler operating from 2 to 18 GHz with 16 dB coupling. Model 1816 was the first commercial product designed using Russell's CAE program. KRYTAR designed and manufactured couplers for their first 18 years in business, then introduced their first power dividers in 1993. Over their past 50 years in business, the company has expanded the product line to include directional couplers, directional detectors, 3 dB hybrids, matched line directional dividers (MLDD) power dividers, detectors, terminations, coaxial adapters, bias tees, Butler matrices, Butlers with phase shift and monopulse comparators. KRYTAR's product family spans from DC to 110 GHz with plans to increase frequency as the industry grows.

KRYTAR products are designed and manufactured in the U.S, and they were awarded a multitude of quality certifications in 2009, which they still maintain. The corporation has comprehensive electrical, mechanical and test documentation standards and follows AS9100D standards, IPC-A-600 PCB workmanship, ISO 9001 quality management and MIL-STD-202 and MIL-STD-810 test methods. KRYTAR also offers environmental validation, including temperature, vibration, shock, vacuum and radiation testing.

KRYTAR began offering space-qualified products in 2012 and has expanded its space product line since. Products manufactured for space and thermal vacuum applications undergo additional reliability and quality assurance inspections during all phases of manufacturing, evaluation and environmental testing. Parts, materials and processes are fully traceable from raw materials to top-level assemblies. Using materials optimized for extreme cold temperature operating environments, KRYTAR began offering components for quantum computing and space applications in 2016. As the industry moves to harsher environments and higher frequencies, KRYTAR is meeting each challenge and continues to design and manufacture new products to meet the growing needs.

KRYTAR is located in Sunnyvale, Calif., the center of Silicon Valley. It is a privately held company, which is becoming rare, and thrives on pillars of technical excellence and customer satisfaction. KRYTAR supports its customers with custom and COTS products available on short timelines. Whether designing wireless networks, serving the satcom industry, advancing defense systems or exploring space, KRYTAR delivers off-the-shelf and custom solutions designed to meet specific needs with precision, quality and reliability.

This year, KRYTAR is celebrating its 50-year anniversary and showing appreciation for clients' trust over the years, which has been built on KRYTAR's ability to meet challenges and deliver results.

https://krytar.com/